

# **Mercury Control with Calcium-Based Sorbents and Oxidizing Agents**

## **Quarterly Report**

Period of Performance:

**April 1<sup>st</sup>, 2003 through June 30<sup>th</sup>, 2003**

**Prepared by**

Thomas K. Gale

July 2003

**DE-PS26-02NT41183**

**Southern Research Institute**

2000 Ninth Avenue South

P. O. Box 55305

Birmingham, AL 35255-5305

**Prepared for**

Barbara Carney

National Energy Technology Laboratory

United States Department of Energy

626 Cochrans Mill Road

Pittsburgh, PA 15236-0940

## Disclaimer

This report was prepared as an account of work sponsored by an agency of the United States Government. Neither the United States Government nor any agency thereof, nor any of their employees, makes any warranty, express or implied, or assumes any legal liability or responsibility for the accuracy, completeness, or usefulness of any information, apparatus, product, or process disclosed, or represents that its use would not infringe privately owned rights. Reference herein to any specific commercial product, process, or service by trade name, trademark, manufacturer, or otherwise does not necessarily constitute or imply its endorsement, recommendation, or favoring by the United States Government or any agency thereof. The views and opinions of authors expressed herein do not necessarily state or reflect those of the United States Government or any agency thereof.

## Abstract

The complicated chemistry and multiple mechanisms affecting mercury speciation and capture make it necessary to investigate these processes at conditions relevant to full-scale boilers. Experiments were performed in a 1MW semi-industrial-scale, coal-fired facility, representative of a full-scale boiler. Southern Research Institute's spike and recovery system and procedures were used to obtain real-time gas-phase mercury-speciation measurements, with less than 5% uncertainty in the measured values. The focus of this work was on solutions for Powder River Basin (PRB) sub-bituminous coals. The results from last quarter indicated that ash composition was more important than chlorine content to Hg-speciation and capture, and the catalytic material in bituminous ash enhances Hg-oxidation and capture by calcium (i.e., PRB flyash and hydrated lime). The results from this quarter prove that unburned carbon (UBC) is the dominant catalytic material of importance in the flyash. Hence, other than UBC and to a lesser extent chlorine, other flue-gas components are relatively unimportant to mercury oxidation and capture.

Sodium tetrasulfide injection in front of a baghouse for mercury control was investigated this quarter with great success! A flue-gas concentration of ~10 ppmv  $\text{Na}_2\text{S}_4$  was sufficient to achieve 100% +/- 2% vapor-phase mercury removal across a baghouse, while firing PRB coal. PRB coal flue gas is problematic in terms of eliminating mercury emissions. Sodium tetrasulfide injection is perhaps the most promising technology to date for dealing with Hg-emissions from PRB coal flue gas.  $\text{Na}_2\text{S}_4$ -injection is also effective at removing mercury from bituminous-produced flue gas. However, HCl in the flue gas reduced  $\text{Na}_2\text{S}_4$ -injection effectiveness at removing mercury directly proportional to the chlorine concentration. It is likely that chlorine hinders mercury capture by scavenging previously captured and settled mercury to re-entrain the mercury in the flue gas as  $\text{HgCl}$  or  $\text{HgCl}_2$ . Other than chlorine content,  $\text{Na}_2\text{S}_4$ -injection was not affected by differences in coal type or flue-gas composition in this investigation.  $\text{Na}_2\text{S}_4$ -injection in front of a baghouse creates a significant residual effect, which may allow cost-reduced intermittent injection.  $\text{Na}_2\text{S}_4$ -injection will also be tested for its effectiveness at removing mercury across an ESP. Flue-gas temperatures above 177 °C (350 °F) significantly hinder the effectiveness of  $\text{Na}_2\text{S}_4$ -injection technology, while temperatures as low as 121 °C (250 °F) are favorable.

| Section                                                   | Table of Contents | Page |
|-----------------------------------------------------------|-------------------|------|
| Introduction.....                                         |                   | 4    |
| <u>Mercury Speciation Investigation</u> .....             |                   | 4    |
| <u>Sodium Tetrasulfide Injection Investigation</u> .....  |                   | 5    |
| Experimental .....                                        |                   | 6    |
| <u>Radiant Furnace</u> .....                              |                   | 6    |
| <u>Fuel Preparation</u> .....                             |                   | 7    |
| <u>Burner Assembly</u> .....                              |                   | 7    |
| <u>Convective Sections</u> .....                          |                   | 8    |
| <u>Computer Data Acquisition and Control System</u> ..... |                   | 8    |
| <u>CEM System for Flue-Gas Composition</u> .....          |                   | 8    |
| <u>Pollution Control Equipment</u> .....                  |                   | 8    |
| <u>Permit Equipment</u> .....                             |                   | 8    |
| <u>Combustor Operations</u> .....                         |                   | 8    |
| <u>Mercury Semi-Continuous Monitoring System</u> .....    |                   | 9    |
| <u>Spike and Recovery System</u> .....                    |                   | 9    |
| <u>Sampling Locations</u> .....                           |                   | 12   |
| <u>Coal Analysis</u> .....                                |                   | 13   |
| Results and Discussion .....                              |                   | 14   |
| <u>Flue-Gas Component Isolation Investigation</u> .....   |                   | 14   |
| <u>Sodium Tetrasulfide Injection Investigation</u> .....  |                   | 17   |
| Conclusions .....                                         |                   | 21   |
| Future Work .....                                         |                   | 22   |
| References .....                                          |                   | 23   |
| APPENDIX A RUN CONDITIONS AND DATA .....                  |                   | 25   |
| APPENDIX B SODIUM TETRASULFIDE INJECTION EQUIPMENT .....  |                   | 31   |
| APPENDIX C UBC VERSUS LOI .....                           |                   | 34   |

| Figure | List of Figures                                                                                            | Page |
|--------|------------------------------------------------------------------------------------------------------------|------|
| 1      | Combustion Research Facility (CRF) .....                                                                   | 6    |
| 2      | Temperature/time history comparison .....                                                                  | 7    |
| 3      | Mercury monitoring system, including spike and recovery .....                                              | 10   |
| 4      | Mercury speciation data taken with an advanced and customized .....                                        | 11   |
| 5      | Vertical duct section used for Na <sub>2</sub> S <sub>4</sub> -injection tests .....                       | 12   |
| 6      | Isolated effect of SO <sub>2</sub> -injection on gas-phase Hg-concentrations .....                         | 14   |
| 7      | Isolated effect of UBC on elemental mercury concentration .....                                            | 15   |
| 8      | Isolated effect of UBC on mercury capture by flyash .....                                                  | 16   |
| 9      | Impact of Na <sub>2</sub> S <sub>4</sub> -injection on gas-phase mercury removal .....                     | 17   |
| 10     | Effect of chlorine on Na <sub>2</sub> S <sub>4</sub> -injection for Hg-emission control .....              | 18   |
| 11     | Effect of temperature on gas-phase Hg-removal by Na <sub>2</sub> S <sub>4</sub> -injection .....           | 19   |
| 12     | Residual effect of Na <sub>2</sub> S <sub>4</sub> -injection on gas-phase Hg-removal across baghouse ..... | 20   |

## Introduction

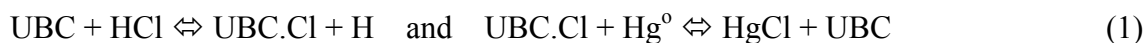
### Mercury Speciation Investigation

The predominant forms of mercury in coal-fired flue gas are elemental ( $\text{Hg}^0$ ) and oxidized ( $\text{HgCl}_2$ ) [1-3]. The percentage of oxidized mercury in the stack effluent of a particular power plant depends on the coal type, combustion efficiency, and the pollution control equipment used. Essentially all of the mercury entering the furnace with the coal is vaporized and exists in the elemental form until the flue gases cool below 1000 °F [1-3]. The oxidation of mercury in coal-fired boiler systems is kinetically limited [1-3]. Because the concentration of mercury is very small in flue gas, any favorable mercury-oxidation reaction does not have the ability to promulgate itself. In virtually every conceivable competitive reaction, the competing gas component, much in excess of mercury, dominates. On the other hand, where the formation of mercuric compounds is thermodynamically favored, the kinetically controlled oxidation is generally slow unless the oxidant is in vast abundance compared with mercury.

In addition to the trace nature of mercury in coal-fired boilers, favorable reactions for mercury oxidation have short temperature/time windows. Consequently, the extent of mercury oxidation is highly dependent on catalytic processes. Heterogeneous catalysis enhances mercury oxidation reactions in two ways. First of all, disperse solid catalytic material provides sorption sites upon which reactions may take place. In addition, heterogeneous catalysis enhances mercury oxidation by effectively making available gas components (such as  $\text{Cl}^*$ ) that are otherwise scavenged by competing gas species present at much higher concentrations. The combination of factors affecting mercury speciation in coal-fired boilers makes it extremely difficult to design a cost-effective strategy for mercury control. The present work attempts to obtain an understanding of the mechanisms governing mercury speciation and capture in flue-gas environments that exist in full-scale utilities. The greater understanding of mercury kinetics will be used to design strategies to enhance capture of mercury by flyash, using additives or via coal-blending, and will aid in calcium-based sorbent optimization for Hg-removal.

A system of reactions, which include significant chlorine-speciation reactions, has been proposed to describe homogeneous Hg-oxidation [4]. This set of governing reactions allows direct oxidation of  $\text{Hg}^0$  to  $\text{HgCl}$  and  $\text{HgCl}$  to  $\text{HgCl}_2$  by the following four chlorine species with different reaction rates:  $\text{Cl}$ ,  $\text{Cl}_2$ ,  $\text{HCl}$ , and  $\text{HOCl}$  [4]. This system of equations has been shown to effectively predict mercury speciation for specific homogeneous systems [2]. However, the homogeneous model alone consistently under predicts the oxidation of mercury from coal-fired boilers [5]. Hence, it is important to identify and describe the heterogeneous reactions that dominate the mercury-oxidation process.

Benchscale work has identified several components of flyash that may play an important role in heterogeneous Hg-oxidation reactions [6-7], particularly unburned carbon (UBC) and iron [7]. Niksa et. al. [8] suggested a possible mechanism whereby UBC can catalyze mercury oxidation, as follows:



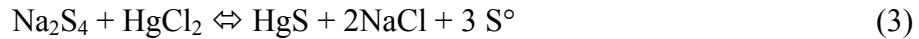
As published in the March03 Quarterly Report [9], an extensive investigation of the differences between Powder River Basin (PRB) coal and Hv-bituminous coals has identified the parameters responsible for differences in mercury speciation and capture. PRB coals produce high-calcium,

low-UBC, and low-iron flyash. They also produce lower sulfur, lower chlorine, and lower NO<sub>x</sub> flue-gas than bituminous coals. In the February03 tests, the list of parameters responsible for these differences were narrowed down to SO<sub>2</sub>, minerals in the ash (i.e., iron content and availability), and UBC [9]. It was not clear from the results whether one, two, or all three of these parameters were responsible for the mercury oxidation and capture enhancement. Isolating parameter experiments were performed in April and May to shed greater light on this subject.

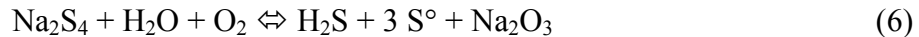
### Sodium Tetrasulfide Injection Investigation

Previous pilot-plant tests have shown sodium tetrasulfide injection to be an effective means of eliminating mercury emissions from Municipal Waste Combustors (MWC) [10]. These MWC tests were performed in conjunction with dry scrubbers, which helped to remove some of the acid gas. In addition, there are 6 commercially operating MWC plants that use Na<sub>2</sub>S<sub>4</sub>-technology to remove mercury. The success of this technology with MWC applications provide evidence that sodium tetrasulfide injection, in conjunction with calcium-based sorbents may also be a favorable technology for Hg-control in coal-fired boilers.

In April 2003, the ability of sodium tetrasulfide to enhance mercury removal from coal-fired flue gas (in conjunction with calcium-based sorbents such as hydrated lime) was examined in the CRF at SRI. According to Licata and Fey [11], sodium tetrasulfide (Na<sub>2</sub>S<sub>4</sub>) decomposes in flue gas into elemental sulfur (S<sup>0</sup>) and ionic sulfide (S<sup>-2</sup>). The elemental sulfur then reacts directly with elemental mercury to form mercuric sulfide, and the ionic forms of sulfur react with ionic mercury to again form mercuric sulfide. Equations (2-3) give examples of these mercury stabilization reactions:



Thermal decomposition alone is sufficient to produce a large independent concentration of elemental sulfur vapor. However, higher temperatures also enhance reactions competing to deplete the injected and generated concentrations of Na<sub>2</sub>S<sub>4</sub>, H<sub>2</sub>S, and elemental sulfur, to form Na<sub>2</sub>SO<sub>3</sub> and SO<sub>x</sub>. Reactions that enhance the decomposition of sodium tetrasulfide include equations (5) and (6) below:



As shown in Equ. (5), chlorine may enhance the decomposition of sodium tetrasulfide. However, since chlorine is highly reactive and the thermodynamically favored mercury species is HgCl<sub>2</sub> in coal-fired flue gas [1], chlorine may also scavenge previously captured mercury in the HgS form. This may be especially true if the HgS is settled in a baghouse filter cake. Hence, chlorine may re-suspend mercury in the flue gas by the reverse of the reaction described by Equ.(4) or by other reactions. Re-entrainment reactions may be quite significant in the filter

cake, especially if they are enhanced by catalysis, analogous to that represented in Equ. (1). Consequently, the impact of chlorine in conjunction with  $\text{Na}_2\text{S}_4$ -injection was also investigated in this work.

## Experimental

The Combustion Research Facility (CRF) at Southern Research Institute (SRI) in Birmingham, AL, is a 1-MW<sub>t</sub> semi-industrial-scale, coal-fired facility, which mimics the thermal profile of a full-scale boiler from the burner through the economizer. Figure 1 shows a two-dimensional sketch of this facility.

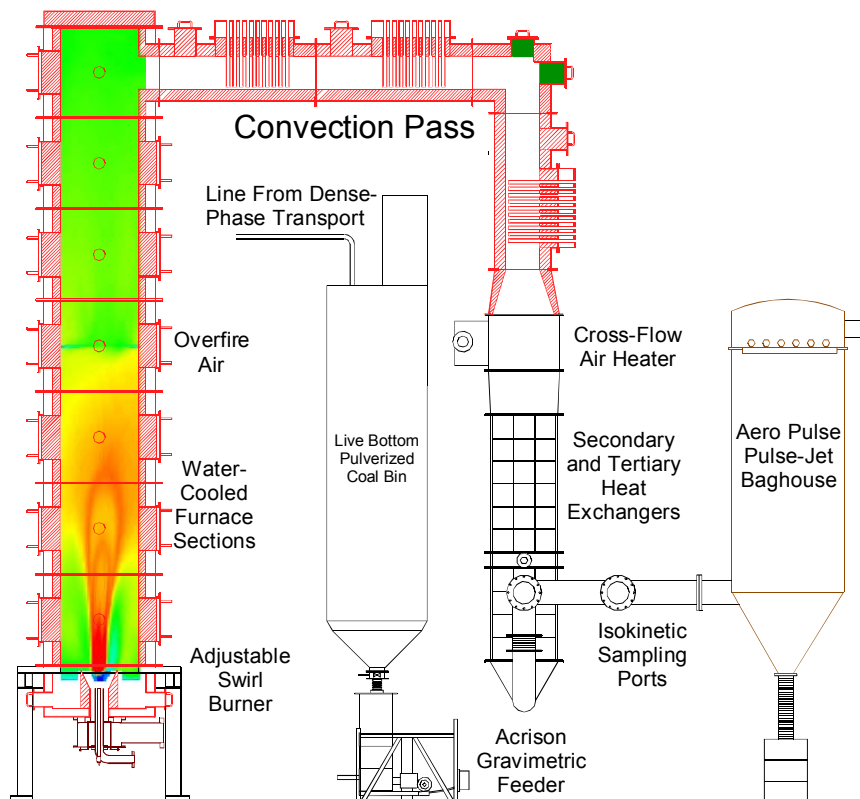


**Figure 1.** Combustion Research Facility (CRF).

### Radiant Furnace

The furnace is a vertical, up-fired, 28-foot high cylinder, with an inner diameter of 3.5-feet (see Figure 1). This allows gas velocities of 10 to 20-feet per second and residence times of 1.3 to 2.5 seconds, depending upon the firing rate. The design furnace exit gas temperature is 2200 °F. As shown in Fig. 2, the temperature/time history of the CRF mimics that of full-scale power plants from the burner through the economizer.

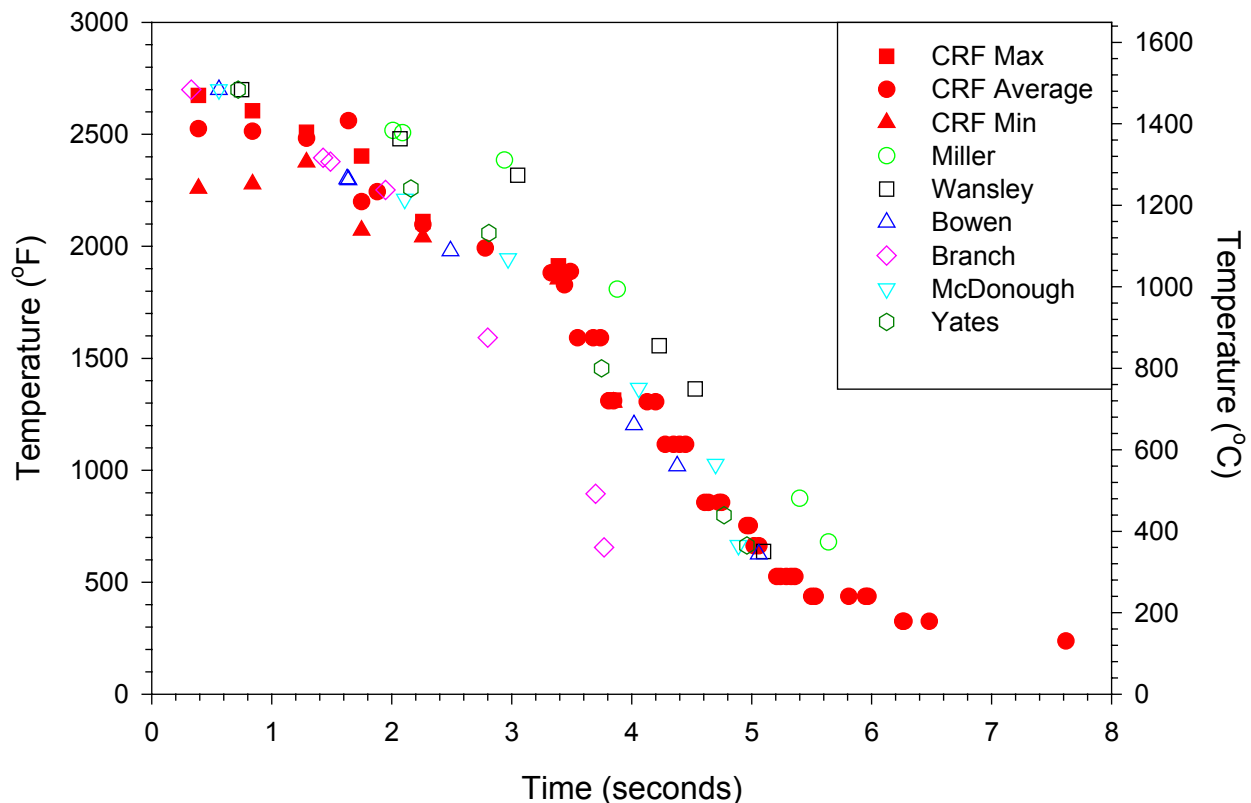


**Figure 2.** Combustion Research Facility (CRF) temperature/time histories compared with those of full-scale Southern Company coal-fired power plants.

### Fuel Preparation

The fuel preparation area includes an open area storage yard, covered on-site storage bins, a rotary drum coal crusher, a CE Raymond bowl mill, and pulverized coal storage. The coal mill is a refurbished and instrumented Model 352 CE-Raymond bowl mill, which has a rated capacity of 2 tons per hour. This type of mill should give representative milling simulations of the different air-swept table and roller mills normally used in power plant service.

### Burner Assembly

The burner is mounted coaxially on the bottom of the furnace and is up-fired using natural gas, pulverized coal, any combination of the two or any other fuel that can be finely divided and transported to the pulverized coal silo. It is equipped with a flow control system for secondary air flow and a set of registers, which impart swirl to the secondary air, separate from the flow control. The secondary air and the primary air-coal mixture enter the furnace through a refractory quarl with a 25° half angle. Two clean-out ports are provided in this section, to allow bottom ash to be periodically removed from the furnace. A closed-circuit television camera with a control-room monitor allows constant monitoring of the view of the flame from the top of the furnace. A low NO<sub>x</sub> firing system, consisting of a generic dual-register burner and an overfire air system, can be installed to simulate several combinations of low NO<sub>x</sub> firing. The single-register burner was used for all experiments in the present investigation.

## Convective Sections

The combustion gases exit the vertical furnace through a horizontal convection pass, which is designed to remove a substantial part of the heat from the flue gases. The extraction of heat was designed to simulate the time-temperature profile found in a utility boiler. A series of three air-cooled tube banks are installed in the convective pass, and the air cooling is used to control either the temperature profile of the flue gases or the tube metal surface temperatures for fouling/ash deposition studies. A cross-flow tubular air preheater follows the convective tube banks and is used to preheat the primary and secondary air. Finally, four air-to-flue-gas recuperators are used to cool the flue gas down to a nominal 149 °C (300°F) before the flue gas enters the pollution control devices.

The convective section is 1.5 feet x 1.5 feet x 22 feet, providing gas velocities of 10 to 20 m/s (30 to 60 ft/s) and residence times of 0.4 to 0.8 seconds, again depending upon the firing rate. The design temperature range for the convective section is 1200 to 650°C (2200 to 1200°F).

## Computer Data Acquisition and Control System

The facility is controlled and monitored by networked combined digital control system (DCS) and data acquisition computers, managed by Yokogawa CS-1000 system software that runs under the Windows NT operating system. This DCS performs all process control for the facility and allows complex feed-forward and calculated variable control. This computer control also performs the monitoring needed for safe operation of combustion equipment, including flame scanning and interlocks, automatic startup, and automatic shutdown of the entire facility. Process data acquisition and storage is accomplished within the Yokogawa software.

## CEM System for Flue-Gas Composition

An extractive continuous-emissions monitoring (CEM) system measured the concentrations of CO, CO<sub>2</sub>, NO<sub>x</sub>, SO<sub>2</sub>, and O<sub>2</sub> in the flue-gas exhaust. In addition, manual measurements of chlorine and moisture were obtained throughout the testing.

## Pollution Control Equipment

Test equipment available for use at the Combustion Research Facility include an Electrically Stimulated Fabric Filter, a dry wall Electrostatic Precipitator, and a fluidized semi-dry / dry desulfurization system.

## Permit Equipment

Particulate emissions are controlled by an Aeropulse pulse-jet baghouse, while sulfur dioxide emissions are controlled by an Indusco packed-column caustic scrubber. The pulse-jet baghouse and scrubber are required for the air quality permit of the facility issued by the Jefferson County Board of Health and are always on-line.

## Combustor Operations

A routine facility operation is usually completed in one week, beginning at 8:00 am on



Monday morning and ending at 5:00 PM on Friday afternoon. To facilitate start of testing on Monday morning the furnace is usually started on Sunday evening, firing with natural gas to heat up the system before switching to coal. It usually requires 12 hours before thermal equilibrium is achieved. The facility is operated 24 hours a day by two 12-hour shifts, during a test week.

### Mercury Semi-Continuous Monitoring System

Mercury monitoring was performed with an advanced and improved version of the PS Analytical 10.665 Stack Gas Analyzer. The PSA monitor has been customized to use an APOGEE Scientific QGIS probe for sampling flue gas. The QGIS probe is designed to pull a large volume of flue gas through an annulus within the probe at a high and turbulent velocity, thus scouring clean the walls of this annulus. The inner wall of the annulus contains a section with a porous frit through which a small sample of flue gas is drawn. The excess flue gas is directed back into the duct, downstream of the sample inlet. In this way, the QGIS probe allows a sample to be drawn from the duct without pulling it through an ash layer, thereby minimizing alteration of the gas sample – especially capture or oxidation of the vapor phase mercury by or on the particulate. Southern Research also developed an advanced *spike and recovery* system to validate the correctness of the mercury-speciation numbers measured and correct for errors that occur. Because of these and other modifications, Southern Research Institute can now measure mercury speciation within a maximum uncertainty of 5%. Accurate and precise mercury speciation measurements are key to fundamental mercury speciation and capture investigations.

### Spike and Recovery System

The *spike and recovery system* is a first of its kind prototype provided by PS Analytical. The adaptation of this *spike and recovery* system to allow spiking at the tip of the APOGEE Scientific QGIS probe was performed by Southern Research personnel. The spike of mercury is introduced into the tip of the APOGEE Scientific QGIS probe far enough downstream from the inlet to prevent losses to the duct and far enough upstream of the porous annulus to allow complete mixing before the sampled gas is pulled through the porous frit. A relatively small quantity of air is used to carry the mercury spike to the probe. Therefore, dilution is insignificant, and the general flue-gas composition is undisturbed. The main impact of the spike is simply to increase the concentration of mercury in the sampled gas. This is significant, since mercury-oxidation processes that interfere with speciation measurements can involve three and four component interactions of flue-gas species on catalytic ash sites [12].

The concentration of mercury in the spike stream is generated by controlling the flow rate, pressures, and temperatures of air in and through a mercury reservoir. In addition, SRI uses a parallel Hg-source for the *spike and recovery* system, involving permeation tubes, allowing a check on the source calibration. High-precision mass-flow controllers are used to obtain the precise metering needed for high-certainty calibrated spikes. The proper use of *spike and recovery* provides a greater level of confidence in the resulting mercury speciation measurements than other methods currently in use. A schematic of the monitoring system is presented in Fig. 3, including spike location, gas-conditioning system, and calibrated spike source.

Figure 4 illustrates the use of the *spike and recovery system* for establishing total and oxidized mercury concentrations in the flue gas, while first burning natural gas (time 0:00 to 5:00) and then Black Thunder, a Powder River Basin (PRB) coal. As shown, the *spike*

recoveries are observed on top of the measured initial mercury concentrations for both fuels.

The mercury speciation data were obtained well upstream of the baghouse. Table 1 contains the Hg-speciation measurements of the PRB flue gas, after correction using the *spike recoveries* shown in Table 2 (explained below).

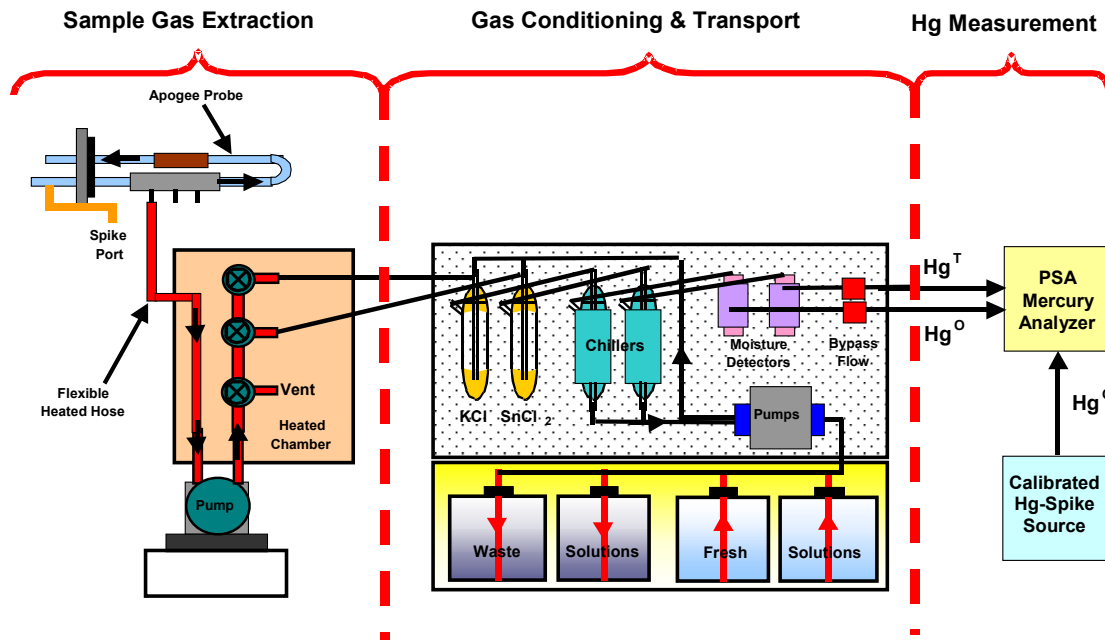


**Figure 3.** Mercury monitoring system, including spike and recovery.

**Table 1.** Location and speciation of Hg-measurements, while firing PRB coal (see Fig. 4).

| Location            | Temperature<br>°C (°F) | Hg <sup>0</sup><br>(μg/Nm <sup>3</sup> ) | Hg <sup>T</sup><br>(μg/Nm <sup>3</sup> ) | Elemental<br>Fraction % |
|---------------------|------------------------|------------------------------------------|------------------------------------------|-------------------------|
| After Recupatherm 1 | 260 (500)              | 7.4 +/- 0.93                             | 8.4 +/- 1.1                              | 88.1 +/- 1.5            |
| After Recupatherm 2 | 163 (325)              | 6.5 +/- 0.44                             | 8.0 +/- 0.70                             | 81.3 +/- 1.0            |

- The mercury concentrations were measured with 6% oxygen in the flue gas.

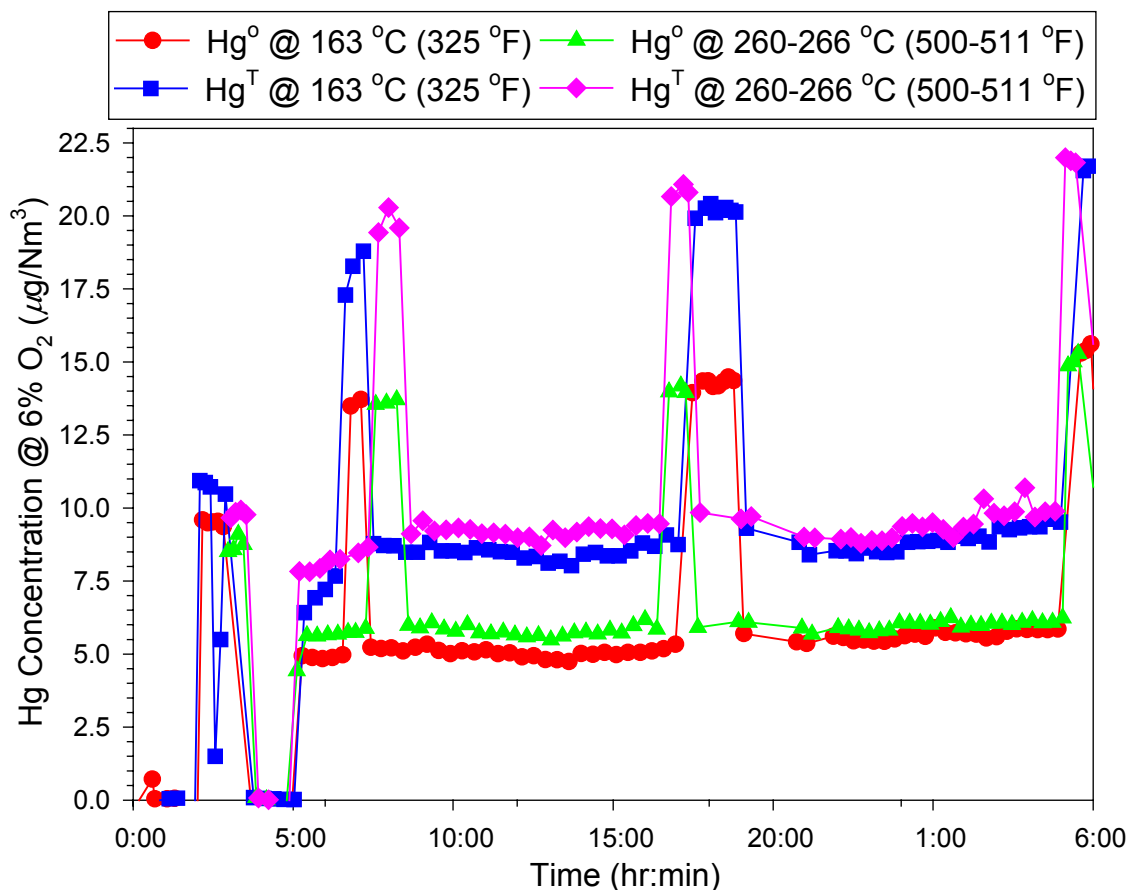
The percentage of elemental mercury was measured directly (i.e., the population of individual measurements of Hg<sup>0</sup> and Hg<sup>T</sup>, taken one after the other, were used to obtain the average and standard deviation for the elemental fraction), not calculated from the other values in the table.

As shown in Table 2, the recoveries of the elemental-mercury spike are consistently lower than the recoveries of total mercury. This is due to undesired oxidation in the Apogee Probe and sampling lines. On the other hand, the stannous chloride (total Hg) impingers scavenge a significant quantity of CO<sub>2</sub>, thus artificially raising the concentration of mercury in the sample gas. However, with *spike and recovery* these errors can be observed and corrected. In this case (see Table 2), the spike recoveries were all within 20% of the expected value.

**Table 2.** Spike recoveries while firing PRB coal.

| Sample Type     | Temperature °C (°F) | Recovery 1 ( $\mu\text{g}/\text{Nm}^3$ ) | Recovery 2 ( $\mu\text{g}/\text{Nm}^3$ ) | Recovery 3 ( $\mu\text{g}/\text{Nm}^3$ ) | Ave Recovery /Spike (%) |
|-----------------|---------------------|------------------------------------------|------------------------------------------|------------------------------------------|-------------------------|
| Hg <sup>o</sup> | 163 (325)           | 8.30                                     | 8.78                                     | 8.06                                     | 86.4                    |
| Hg <sup>T</sup> | 163 (325)           | 10.96                                    | 11.13                                    | 10.80                                    | 113.0                   |
| Hg <sup>o</sup> | 260 (500)           | 7.91                                     | 8.24                                     | 7.81                                     | 82.4                    |
| Hg <sup>T</sup> | 260 (500)           | 11.59                                    | 11.64                                    | 11.06                                    | 117.8                   |

- The Hg<sup>o</sup> spike injected into the tip of the sampling probe was  $\sim 9.7 \mu\text{g}/\text{Nm}^3$ .

**Figure 4.** Mercury speciation data taken with an advanced and customized semi-continuous monitor and validated with *spike and recovery* for quality assurance.

Hence, a simple linear correction factor was used. As partially apparent in the data of Table 2, the difference in recoveries between expected and actual values was systematic, not random. In addition, as apparent in Fig. 5, there was little variation of the measured data for the flue-gas measurements or the spike-recoveries themselves. Using the *spike and recovery system* to correct for the systematic error has allowed mercury speciation measurements with less than 5% uncertainty for all of the data presented in this report. This estimate of uncertainty is the standard deviation of corrected values added to the inherent uncertainty of the measurement technique.

Tables 3-5 contain the analysis (including Hg and Cl) of the Black Thunder Powder River Basin Coal (PRB) and the two bituminous coals, Choctaw America and Blacksville, used in this

work. The PRB coal is the same coal used to obtain the data in Fig. 5. As shown in Tables 3 and 4, both PRB and Choctaw America are low chlorine coals. Blacksville is a higher chlorine coal (see Table 5). Choctaw America was chosen to blend with PRB for two reasons. First, it is a low chlorine coal, so the importance of other parameters could more easily be examined without interference of chlorine. Second, it has a high iron content. As shown in Table 6, Blacksville has an even higher iron content than Choctaw America, which is the primary reason for choosing this coal to blend.

For the sodium tetrasulfide injection tests, Choctaw America and Black Thunder (PRB) coals were fired separately to provide a range of coal types. Choctaw America coal (Choctaw) was used to provide a representative bituminous ash and flue gas. Since Choctaw is a low chlorine coal, it was fairly easy to assess the impact of low- and high-chlorine bituminous coals, by performing  $\text{Na}_2\text{S}_4$ -injection tests with and without chlorine addition through the burner. Chlorine gas ( $\text{Cl}_2$ ) was injected through the primary-air line, the impact of which was identical to firing a coal with a higher chlorine-content [1]. The PRB tests were particularly interesting, because  $\text{Na}_2\text{S}_4$ -injection technology has the potential to effectively capture the mercury produced by this problematic (in terms of Hg-emissions) coal. The PRB coal is also very low in chlorine.

### Sampling Locations

For the mercury speciation investigation, measurements were made at the inlet and outlet of an Aero-Pulse pulse-jet baghouse, which uses full-scale Ryton-bags.

For the sodium tetrasulfide tests,  $\text{Na}_2\text{S}_4$ -solution was injected into a 65-foot vertical section of duct at the duct centerline, using heated-air atomization. The injection location was at the bottom of a large U-shaped duct section (each leg was  $\sim 32.5$  feet) that preceded the fabric filter baghouse. Figure 5 contains a schematic of the U-shaped duct section and baghouse used for the sodium tetrasulfide injection tests.

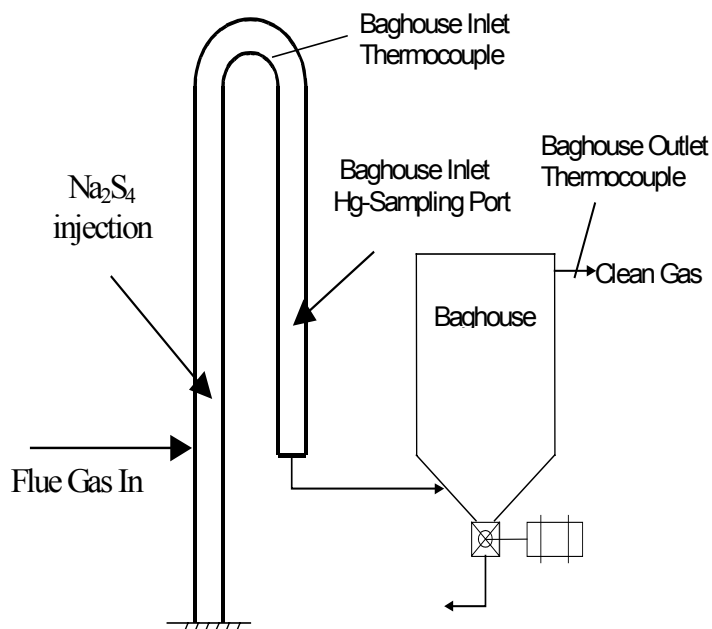


**Figure 5.** Vertical duct section used for  $\text{Na}_2\text{S}_4$ -injection tests.

## Coal Analysis

**Table 3.** Black Thunder PRB Sub-bituminous coal analysis (from coal feeder discharge).

| Proximate Analysis (as rec.) |       | Ultimate analysis (daf) |       | Hg and Cl Analysis (as rec.) |                 |
|------------------------------|-------|-------------------------|-------|------------------------------|-----------------|
| % Moisture                   | 14.00 | % Carbon                | 74.55 | Hg ( $\mu\text{g/g}$ )       | 0.068 +/- 0.005 |
| % Ash                        | 5.92  | % Hydrogen              | 4.78  |                              |                 |
| % Volatiles                  | 37.57 | % Nitrogen              | 1.03  |                              |                 |
| % Fixed C                    | 42.70 | % Sulfur                | 0.37  | Cl (%)                       | < 0.010         |
| HV (Btu/lb)                  | 9,969 | % Oxygen                | 19.27 |                              |                 |

**Table 4.** Choctaw America HvA Bituminous coal analysis (from coal feeder discharge).

| Proximate Analysis (as rec.) |        | Ultimate analysis (daf) |       | Hg and Cl Analysis (as rec.) |                 |
|------------------------------|--------|-------------------------|-------|------------------------------|-----------------|
| % Moisture                   | 2.04   | % Carbon                | 85.39 | Hg ( $\mu\text{g/g}$ )       | 0.065 +/- 0.005 |
| % Ash                        | 4.19   | % Hydrogen              | 5.16  |                              |                 |
| % Volatiles                  | 31.76  | % Nitrogen              | 2.04  |                              |                 |
| % Fixed C                    | 62.01  | % Sulfur                | 0.96  | Cl (%)                       | 0.0127          |
| HV (Btu/lb)                  | 14,019 | % Oxygen                | 6.45  |                              |                 |

**Table 5.** Blacksville HvA Bituminous coal analysis (from coal feeder discharge).

| Proximate Analysis (as rec.) |        | Ultimate analysis (daf) |       | Hg and Cl Analysis (as rec.) |        |
|------------------------------|--------|-------------------------|-------|------------------------------|--------|
| % Moisture                   | 4.03   | % Carbon                | 84.00 | Hg ( $\mu\text{g/g}$ )       | 0.09   |
| % Ash                        | 8.49   | % Hydrogen              | 5.40  |                              |        |
| % Volatiles                  | 37.01  | % Nitrogen              | 1.67  |                              |        |
| % Fixed C                    | 50.47  | % Sulfur                | 3.10  | Cl (%)                       | 0.0580 |
| HV (Btu/lb)                  | 13,299 | % Oxygen                | 5.84  |                              |        |

**Table 6.** Mineral analysis of parent coals (from coal feeder discharge).

| Species                          | Black Thunder | Choctaw America | Blacksville |
|----------------------------------|---------------|-----------------|-------------|
| % Li <sub>2</sub> O              | 0.01          | 0.06            | 0.03        |
| % Na <sub>2</sub> O              | 1.4           | 1.1             | 1.0         |
| % K <sub>2</sub> O               | 0.50          | 2.0             | 2.9         |
| % MgO                            | 4.3           | 1.1             | 1.0         |
| % CaO                            | 22.0          | 2.5             | 4.6         |
| % Fe <sub>2</sub> O <sub>3</sub> | 6.0           | 13.8            | 21.1        |
| % Al <sub>2</sub> O <sub>3</sub> | 15.4          | 31.4            | 21.3        |
| % SiO <sub>2</sub>               | 35.4          | 42.6            | 41.6        |
| % TiO <sub>2</sub>               | 1.3           | 1.3             | 1.2         |
| % P <sub>2</sub> O <sub>5</sub>  | 0.70          | 0.16            | 0.08        |
| % SO <sub>3</sub>                | 11.5          | 2.8             | 4.8         |

## Results and Discussion

### Flue-Gas Component Isolation Investigation

As mentioned earlier, the parameters affecting Hg-speciation in coal-fired flue gas were greatly elucidated in the last quarterly report [9]. Part of this information was also presented at the 2003 MEGA Symposium [13]. The list of parameters responsible for the difference between Hg-speciation and capture in PRB and Hv-bituminous coal flue gas was narrowed down to three, SO<sub>2</sub> concentration, unburned carbon in the ash (UBC), and mineral matter in the ash (i.e., iron form and availability). In addition, the effect of ash composition was isolated in the February test by independently injecting bituminous flyash into the baghouse while firing PRB coal. It was shown that the bituminous ash did enhance mercury oxidation and capture at a constant SO<sub>2</sub> concentration [9].

In April, the impact of SO<sub>2</sub> on Hg-speciation was isolated by injecting SO<sub>2</sub> into the flue gas while burning PRB coal and measuring the elemental and oxidized concentrations of mercury at the front and back of the baghouse. The SO<sub>2</sub> was injected just ahead of the air heater to avoid any additional SO<sub>3</sub> generation. As shown in Fig. 6, essentially no change in elemental or total mercury was observed due to the increase in SO<sub>2</sub> concentration, although the concentration of SO<sub>2</sub> in the flue gas was increased from 204 ppm to 691 ppm. In addition, the measured split between elemental and oxidized mercury, shown in Fig. 6, is consistent with expected values, given the %UBC measured in the ash [9, 13]. Hence, SO<sub>2</sub> concentration is not a parameter that causes mercury-speciation differences between PRB and bituminous flue gases.

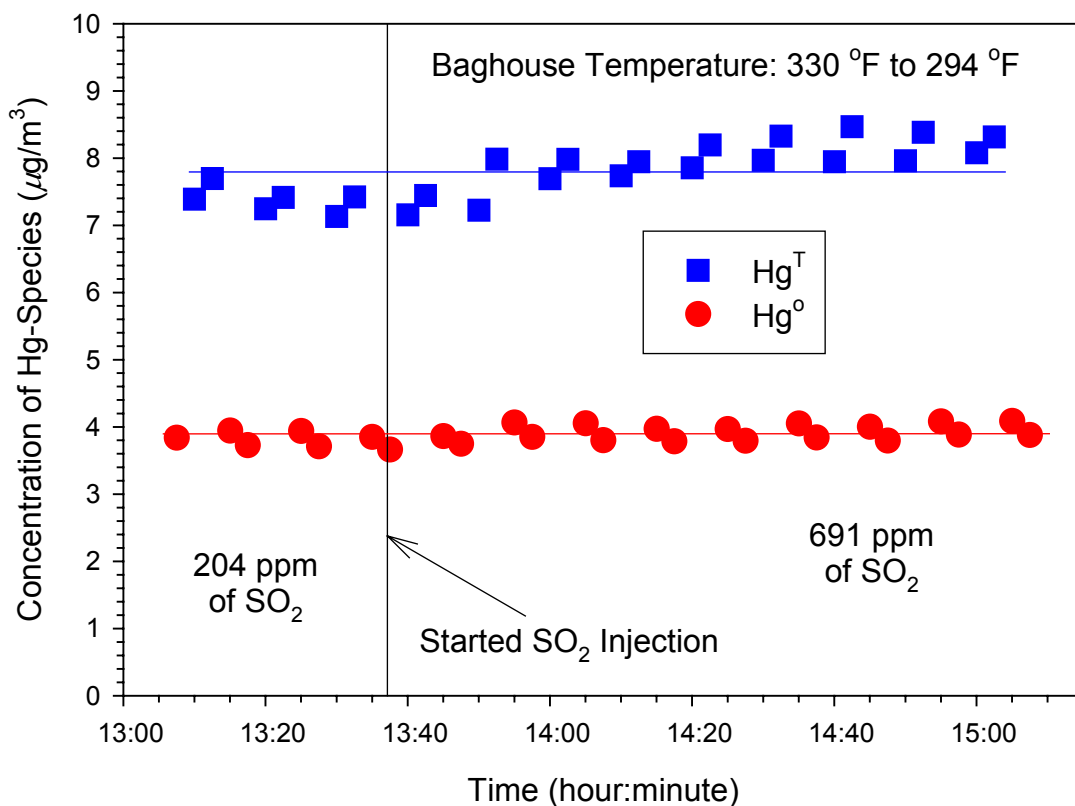


**Figure 6.** Isolated effect of SO<sub>2</sub>-injection on gas-phase Hg-concentrations.

The results of Fig. 6 leave only two parameters to separate, mineral matter (i.e., iron) and UBC. In order to isolate UBC, PRB coal was burned at normal and at extreme firing conditions. The coal was ground coarse; staging with 30% OFA was used (no swirl on the OFA injectors), and the furnace exit oxygen (FEO) was lowered to 1.5%. The flame at the burner was maintained with a high swirl and sufficient oxygen to consume all of the volatiles, so as not to make soot. Since the properties of soot are different than unburned char, it was desirable to increase UBC only by increasing the unburned amount of char in the ash. Figures 7 and 8 contain the results from the UBC isolation tests (funded under the EPRI/EPA Hg-Speciation Program at SRI) along with the data from the coal blending investigation performed in February.

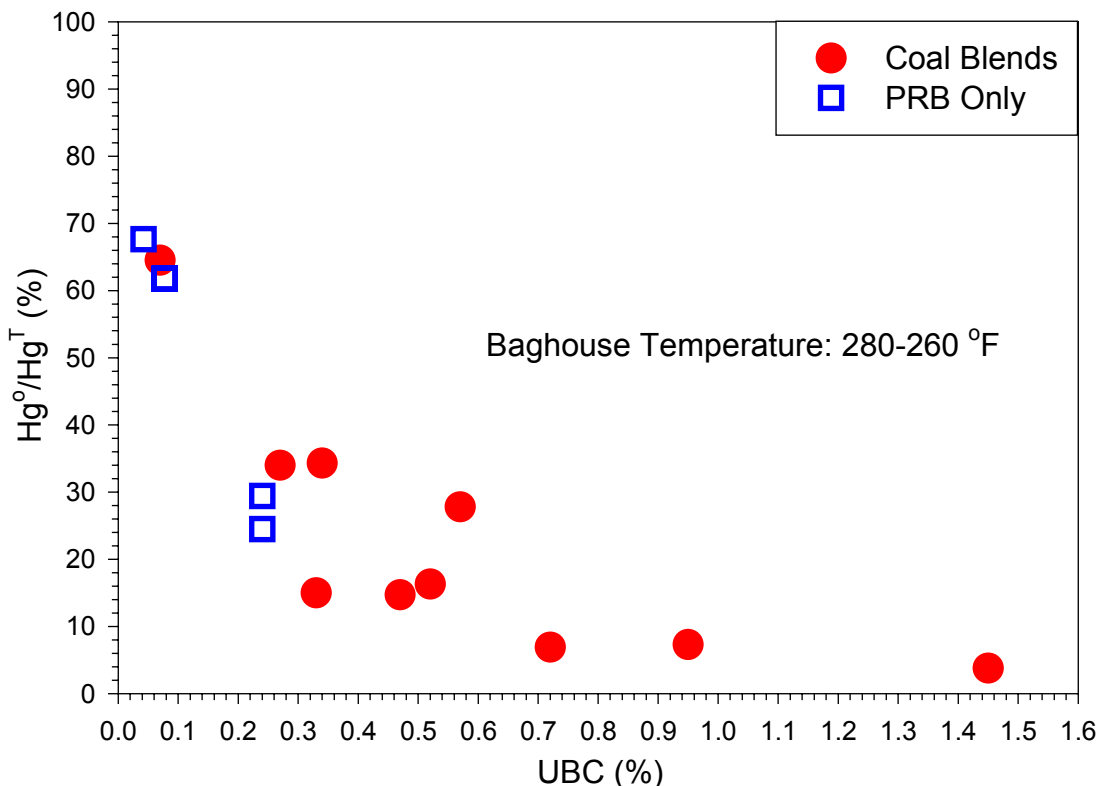


**Figure 7.** Isolated effect of UBC on elemental mercury concentration at baghouse outlet.

Figure 7 shows the effects of UBC on Hg-oxidation. As shown in Fig. 7, UBC was the parameter responsible for the enhanced mercury oxidation observed for the coal blends examined extensively in February (see Earlier Quarterly Report [9]). In fact, the UBC from the isolation tests was a bit more effective at causing mercury oxidation than the increase in UBC due to coal blending. This may be due to the nature of UBC in PRB and Hv-bituminous ash. The carbon in Hv-bituminous ash is generally in separate particles from the mineral particles [14]. However, the amount of UBC in PRB ash is generally less than in bituminous ash and may be more dispersed upon the surface of the mineral particles. Hence, the surface area and/or availability of the PRB UBC may have been greater than the UBC added by blending Hv-bituminous coal with the PRB.

Figure 8 illustrates the relationship between Hg-capture across the baghouse and UBC in the ash. The results from the February test were convoluted, such that it was not certain that the increase in mercury capture was entirely due to an increase in UBC. It was unknown whether or

not the bituminous ash catalytic effect was also due to an increase in the availability of other minerals in the ash, such as iron [9]. However, this quarter's results (see Fig. 8) clearly show that UBC is a dominant parameter affecting Hg-removal. It was previously shown [9, 15] that calcium, either in the PRB ash or injected as  $\text{Ca}(\text{OH})_2$  was an effective sorbent for mercury if it was mixed with a catalyst, such as bituminous ash. Figure 8 shows that UBC was the component in the bituminous ash that was most important in terms of enhancing mercury capture by the calcium in the PRB ash. The mercury removal as a function of UBC has a non-zero y-intercept for the coal blend data. However, the isolated UBC data (no blending, just PRB coal) has a zero y-intercept. Therefore, UBC with PRB-only (increased by altering combustion conditions) is more effective at enhancing mercury removal by the high-calcium ash than the UBC added through coal blending (see Fig. 8).

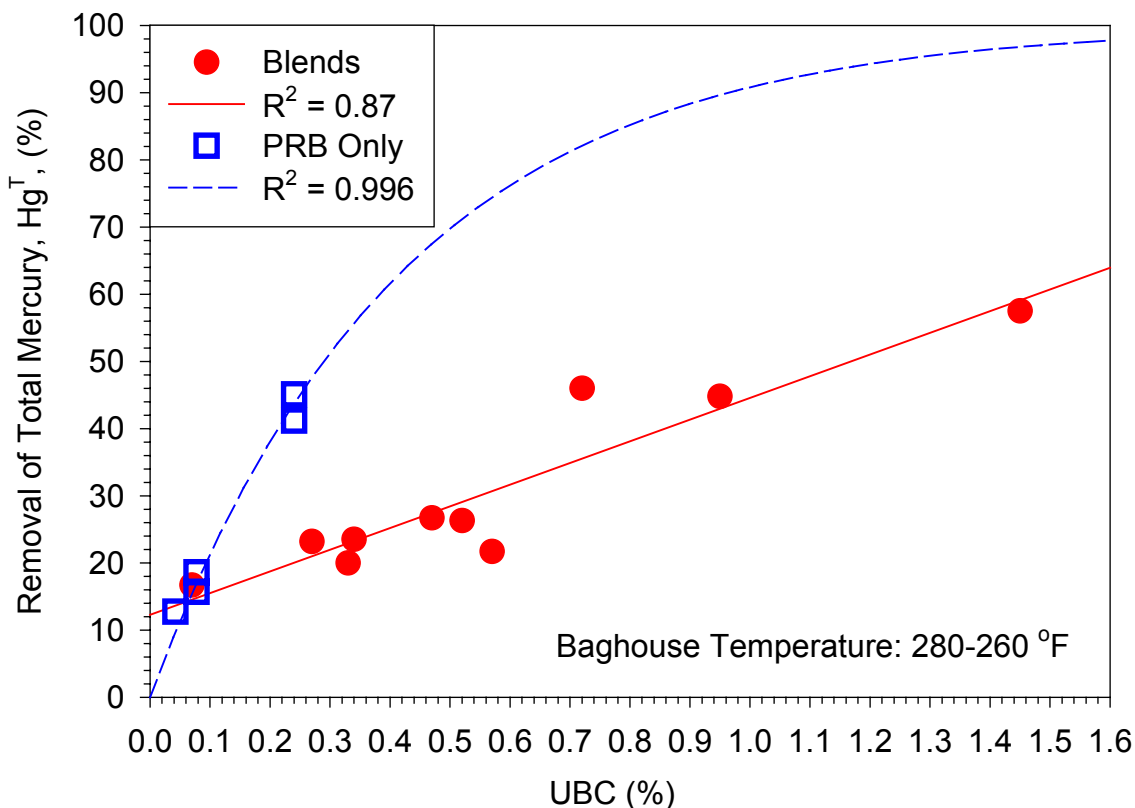


**Figure 8.** Isolated effect of UBC on mercury capture by flyash (measured at baghouse outlet).

There are several reasons for this. First, the UBC added through coal blending carried with it more inert material (i.e., silica and alumina) than the PRB ash. Calcium is also a very important part of the Hg-capture reaction, because calcium is the sorbent material that captures the oxidized mercury [9, 15]. Hence, increasing the UBC through blending with bituminous coal simultaneously decreased the concentration of calcium in the ash. Whereas, increasing the UBC via combustion modifications, while burning PRB coal only, did not significantly decrease the calcium concentration in the ash. Secondly, the UBC in the PRB ash, as discussed above, may be more intimately associated with the high-calcium ash. Thus, the nature of UBC in the PRB ash may make it a more effective catalyst than the UBC in the bituminous coal.

Finally, if the UBC in the PRB ash is more intimately associated with the high-calcium ash than UBC added through coal blending, this may allow a fast and efficient pathway for the



capture of mercury by the high-calcium ash. For example, a thin layer of UBC on the PRB ash particles may provide sites where the mercury is first oxidized and then immediately captured. On the other hand, even the capture of oxidized mercury (i.e.,  $\text{HgCl}_2$ ) may be catalytically enhanced by adsorption on the UBC, followed by capture on the calcium particles.

### Sodium Tetrasulfide Injection Investigation

Figure 9 shows the results of the sodium tetrasulfide injection tests, specifically its effect on mercury removal from the *gas-phase*. *No particulate mercury was measured* in this investigation. At the far left of the graph in Fig. 9 are the data points for the baseline condition, without any  $\text{Na}_2\text{S}_4$  injection. As shown, a significant amount ( $>40\%$ ) of mercury was captured across the baghouse even without  $\text{Na}_2\text{S}_4$  injection. These pre-injection removals were consistent with previously measured values for similar amounts of unburned carbon in the ash [9]. Injection of  $\text{Na}_2\text{S}_4$  caused Hg-removal to increase substantially. In fact, essentially complete ( $100\% \pm 2\%$ ) removal of mercury was obtained while firing PRB coal and injecting sodium tetrasulfide (flue-gas concentration  $\sim 12 \text{ ppmv } \text{Na}_2\text{S}_4$ ).

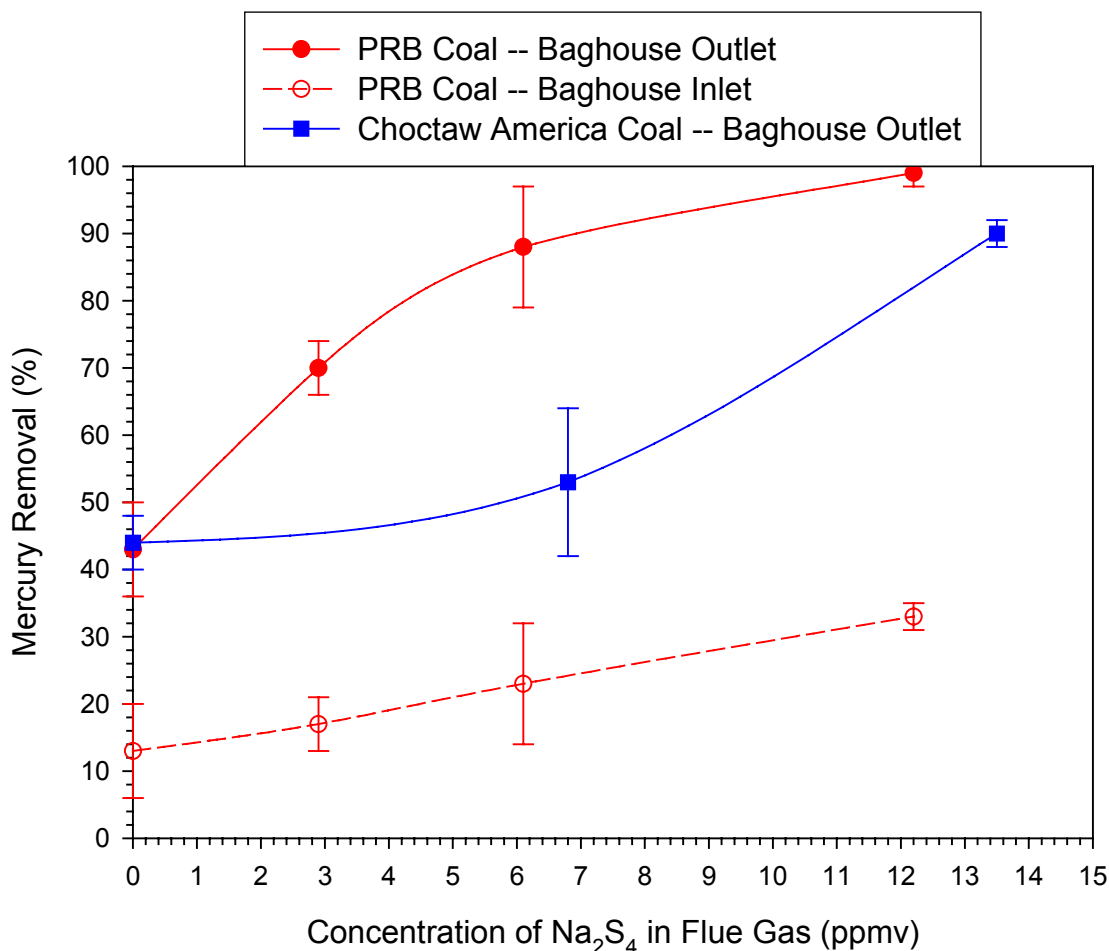


**Figure 9.** Impact of  $\text{Na}_2\text{S}_4$ -injection on gas-phase mercury removal.

Simultaneous injection of calcium-based sorbents and sodium tetrasulfide was planned for this test series. However, the 100% capture result made this an obsolete test condition.

Although calcium-sorbents were not injected during this test, calcium sorbents may play a synergistic role in Hg-removal and/or may remove extra  $\text{H}_2\text{S}$  produced from  $\text{Na}_2\text{S}_4$  injection.

Sodium-tetrasulfide injection was much less successful at removing mercury at the baghouse inlet than at the baghouse outlet. However, the baghouse-inlet measurement location was only 2.0 – 2.5 seconds downstream of the  $\text{Na}_2\text{S}_4$ -injection location. The mercury measurement location downstream of the baghouse was 4.0 – 5.0 seconds from the injection location, in addition to being downstream of the filter cake. There was some Hg-removal prior to the baghouse inlet, and perhaps  $\text{Na}_2\text{S}_4$  would be more effective at removing the mercury from the disperse phase, if more residence time was available. This may be the case for certain ESP applications.

As shown in Fig. 9,  $\text{Na}_2\text{S}_4$  effectively removed the bituminous coal (Choctaw America) mercury from the flue gas, but more  $\text{Na}_2\text{S}_4$  was needed to capture the bituminous mercury than was needed to capture the PRB mercury. Figure 10 illustrates why. Chlorine, more abundant in the bituminous coal, reduced the effectiveness of the  $\text{Na}_2\text{S}_4$ -injection for Hg-removal. Whether the chlorine measured in the flue gas came from the coal or via independent injection through the burner, there is an inverse relationship between mercury removal and chlorine concentration in the flue gas. It is also apparent that for this particular investigation, mercury capture via  $\text{Na}_2\text{S}_4$ -injection technology was essentially unaffected by coal type, other than changes in flue-gas chlorine content, since the relationship between Hg-removal and chlorine concentration is linear, regardless of the source of the chlorine (see Fig. 10).

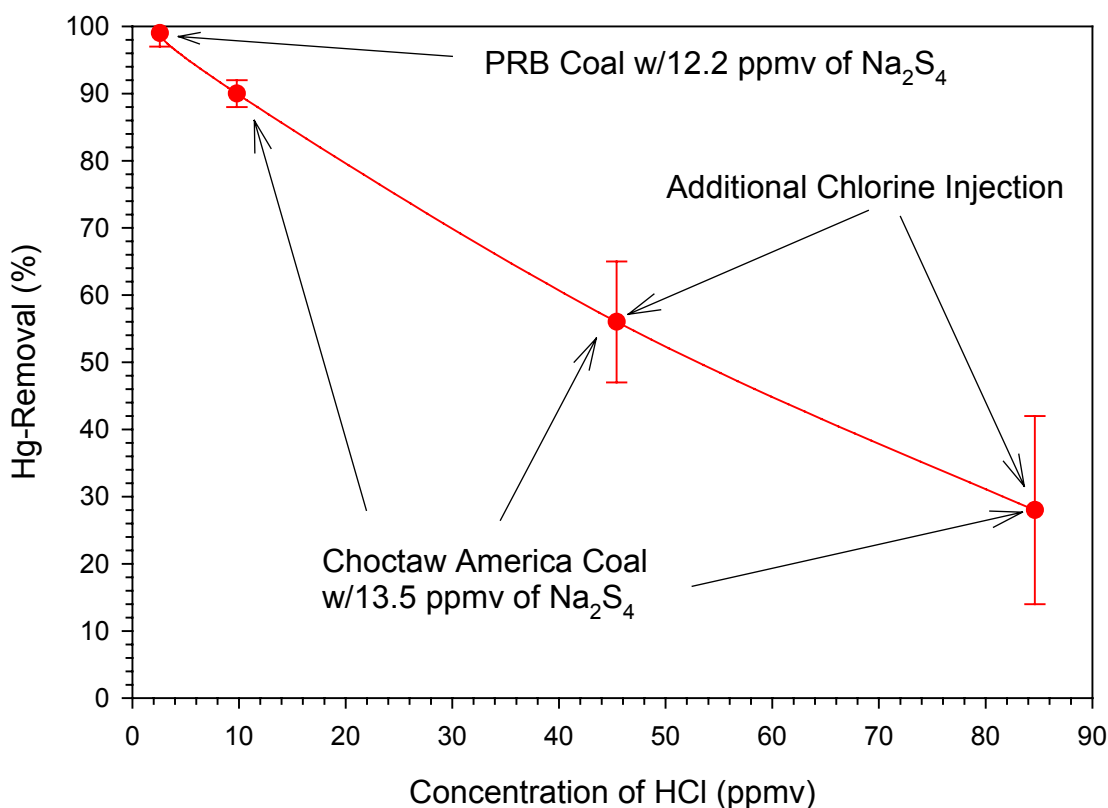


**Figure 10.** Effect of chlorine on  $\text{Na}_2\text{S}_4$ -injection for Hg-removal across the baghouse.

Following the simultaneous chlorine and  $\text{Na}_2\text{S}_4$ -injection tests, the  $\text{Na}_2\text{S}_4$ -injection was turned off and the chlorine left on for several hours. The concentration of total mercury at the

baghouse inlet rose to 1.7 times that of the mass-balance predicted values, thus indicating that previously settled or captured mercury was being scavenged and re-released into the flue gas. It is likely that this was also the mechanism in the baghouse by which chlorine reduced the effectiveness of mercury removal, although the baghouse outlet concentration of mercury was always lower than that of the baghouse inlet.

Figure 11 illustrates the importance of injection temperature on the ability of  $\text{Na}_2\text{S}_4$  to remove mercury, measured at the baghouse outlet. Mercury removal in Fig. 11 is plotted versus the flue-gas temperature into which the sodium tetrasulfide was injected. The temperature values shown in Fig. 11 were obtained by measuring the flue-gas temperature ~32 feet down stream of the  $\text{Na}_2\text{S}_4$ -injection port, which was upstream of the baghouse. The actual temperature of the flue gas at the injection port was probably a bit higher.

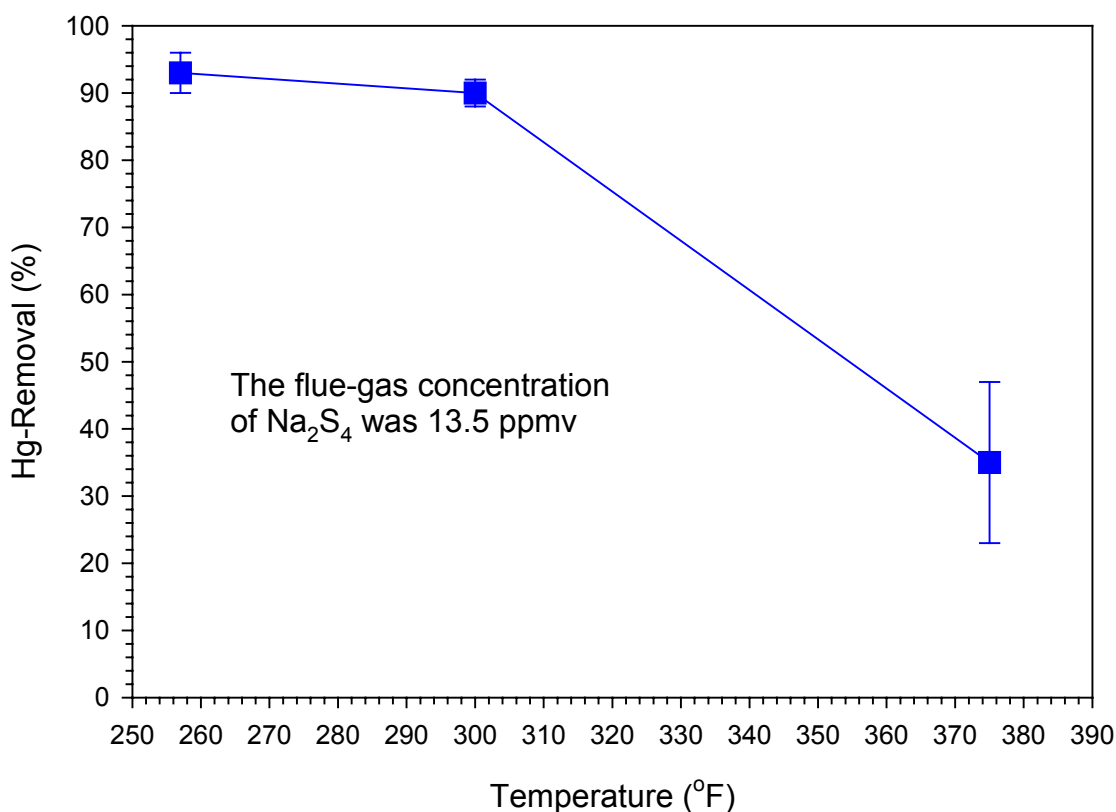


**Figure 11.** Effect of temperature on Hg-removal by  $\text{Na}_2\text{S}_4$ -injection.

Table 7 contains the temperatures measured at three different locations, for the low, medium, and high temperature conditions, respectively corresponding to the data in Fig. 11. In the temperature range investigated, lower temperatures are more favorable for Hg-removal, and temperatures above 177 °C (350 °F) are highly detrimental to mercury removal. The temperature of the air used to inject  $\text{Na}_2\text{S}_4$  was between 170 °C (340 °F) and 180 °C (360 °F) (see App. B). A different air-atomization temperature may change the relationship (see Fig. 11) with flue-gas temperature.

**Table 7.** Gas-temperatures relating to the low, medium, and high temperature tests.

| Location of Temperature Measurement                                                                       | Low Temp. (°F) | Medium Temp. (°F) | High Temp. (°F) |
|-----------------------------------------------------------------------------------------------------------|----------------|-------------------|-----------------|
| Outlet of the last heat exchanger, upstream of the Na <sub>2</sub> S <sub>4</sub> injection port.         | 275            | 325               | 410             |
| U-Duct Elbow, approx. halfway between the Na <sub>2</sub> S <sub>4</sub> injection port and the baghouse. | 257            | 300               | 375             |
| Baghouse outlet duct.                                                                                     | 245            | 273               | 325             |

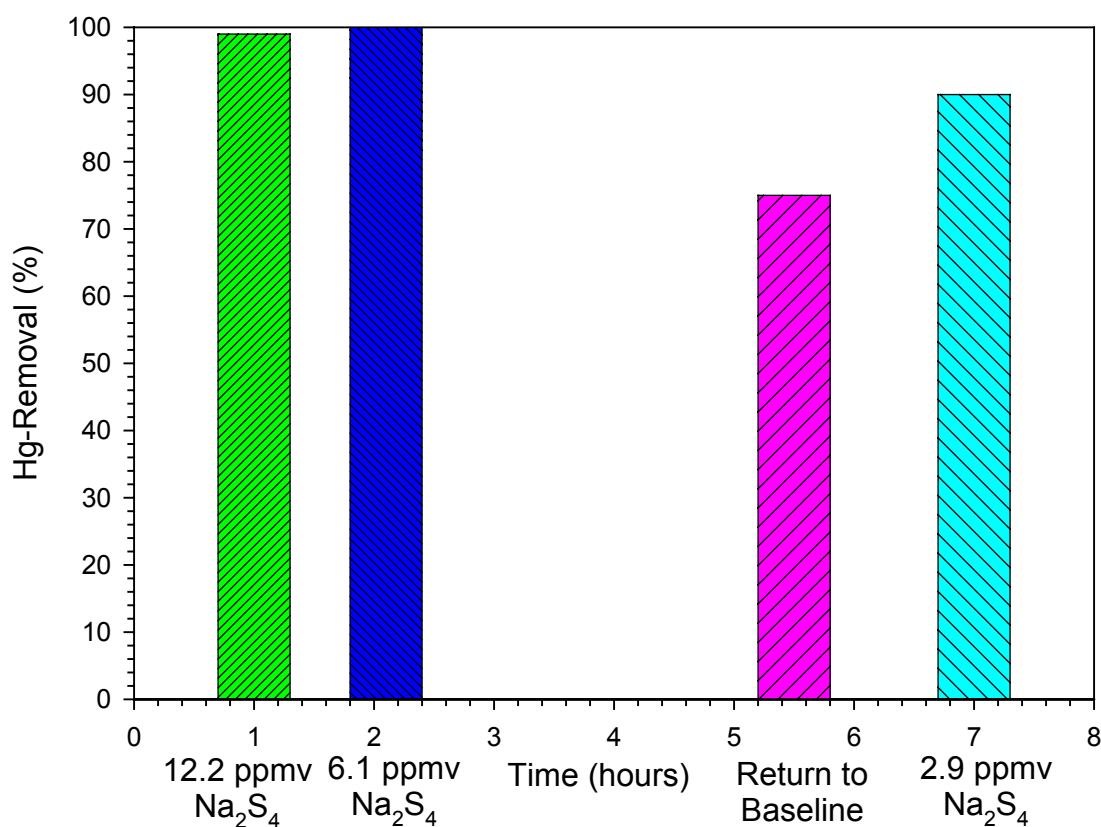
**Figure 12.** Residual effect of Na<sub>2</sub>S<sub>4</sub>-injection on gas-phase Hg-removal across baghouse.

Figure 12 illustrates the residual effect of Na<sub>2</sub>S<sub>4</sub> injection on gas-phase Hg-removal. As shown, at 12.2 ppmv of Na<sub>2</sub>S<sub>4</sub>, nearly all of the mercury was removed while firing PRB coal. However, when the injection of sodium tetrasulfide was reduced by half (to 6.1 ppmv), the mercury removal did not decrease. In fact, the measured mercury removal was 100% +/- 2%. This result indicates a residual effect of the sodium tetrasulfide injection, possibly associated with the baghouse filter cake. The 100% removal is greater than observed for a similar 6.1 ppmv Na<sub>2</sub>S<sub>4</sub>-injection condition, which *did not follow* a higher injection condition (see Fig. 9). As shown in Fig. 9 (an earlier evaluation), the 12.2 ppmv condition would have eventually reached 100% Hg-removal. Lowering the concentration of Na<sub>2</sub>S<sub>4</sub> by half (see Fig. 12) revealed that the

residual effect of the 12.2 ppmv injection rate combined with the 6.1 ppmv actual injection rate combined to yield 100% Hg-removal.

Following the 6.1 ppmv injection rate, the sodium tetrasulfide was turned off and the system was allowed to return to baseline for 3 ½ hours. At the end of this time, the mercury removal measured at the baghouse outlet was still nearly 70% greater than the original baseline condition (see Fig. 9). Following the attempted return to baseline, the sodium tetrasulfide was again injected at an even smaller concentration of 2.9 ppmv. The resulting removal was nearly 90%, much higher than if the residual effect had not been present (see Fig. 9). The data in Fig. 9 indicates that sodium tetrasulfide may be effective at removing mercury in the disperse phase, particularly if there is enough residence time. However, the residual effect illustrated in Fig. 12 is probably associated with the baghouse filter cake. Given the fact that a residual effect is evident, Na<sub>2</sub>S<sub>4</sub>-injection to remove mercury across a baghouse may be very cost effective, since only intermittent injection may be necessary.

Since Na<sub>2</sub>S<sub>4</sub>-injection creates the potential for the flyash to desorb H<sub>2</sub>S vapor, a hand-held H<sub>2</sub>S monitor was used to evaluate the ash samples following the test. Baghouse ash possessed a strong odor following Na<sub>2</sub>S<sub>4</sub>-injection. Baghouse ash samples were taken following injection and immediately sealed in pint cans. These ash samples (both PRB and Choctaw) were found to contain 25-35 ppm of H<sub>2</sub>S in the head space of the cans a day after the samples were collected. Stirring the ash in the cans increased the H<sub>2</sub>S concentration to as much as 75 ppm. In addition, after the gas was evacuated and the cans reclosed and allowed to sit for another day, additional H<sub>2</sub>S was released. Hence, the amount of H<sub>2</sub>S in the ash was significant and was slowly released from the flyash.

Flue gas measurements of H<sub>2</sub>S either before or after the baghouse showed less than 1.0 ppm of H<sub>2</sub>S in the flue gas. Hence, the production of H<sub>2</sub>S should not be a problem when using Na<sub>2</sub>S<sub>4</sub>-injection to control mercury emissions. In addition, flyash samples were tested for H<sub>2</sub>S release with water addition and HCl addition. Qualitative results indicated that H<sub>2</sub>S was not released when ash was submerged in DI-water, and the addition of HCl made little difference.

Samples of baghouse ash were taken after each condition. These baghouse ash samples were subjected to the Toxicity Characteristic Leaching Procedure (TCLP) test. The Hg-concentration of all leachate from all tests of all ash samples was less than half the limiting value of 200 ppb (see Appendix A). Five gallons of ash from the baghouse, containing the mercury captured by means of Na<sub>2</sub>S<sub>4</sub>-injection, have been sent to the National Engineering Technology Laboratory (NETL—Ann Kim's group) for long-term leaching tests. These tests will most likely be performed in the next couple of months. The final tests that need to be performed are the thermal stability tests for mercury desorption and the foaming index test to assure that the flyash produced is acceptable as a cement additive. Data from these analyses will be reported in an upcoming quarterly report.

## Conclusions

- 1) Unburned carbon (UBC) in ash is the overwhelming primary component responsible for the difference observed in vapor-phase mercury speciation between Powder River Basin (PRB) sub-bituminous coal flue gas and bituminous coal flue gas.
- 2) The UBC produced by burning PRB coal is more effective at oxidizing mercury than the UBC produced by burning bituminous coal, on a per mass basis.

- 3) Increased UBC in ash is the primary component responsible for coal-blending enhancement of mercury capture on high-calcium (PRB) ash.
- 4) Unburned carbon enhances mercury capture on calcium by catalytically enhancing mercury oxidation prior to capture. UBC may also enhance Hg-capture by catalytically enhancing the capture of oxidized mercury by calcium. Although the carbon and calcium in flyash are not intimately associated, some contact between the carbon in ash and the calcium does occur, which may provide some opportunity for sorption followed by capture.
- 5) Sodium tetrasulfide injection ( $\sim 10$  ppmv  $\text{Na}_2\text{S}_4$  in flue gas), approximately 2.0 seconds ahead of a baghouse, is sufficient to remove 100%  $\pm$  2% of the flue-gas mercury, while burning a relatively low chlorine coal.
- 6) Injection temperatures above  $177^\circ\text{C}$  ( $350^\circ\text{F}$ ) are detrimental to the effectiveness of  $\text{Na}_2\text{S}_4$ -injection technology, while injection temperatures as low as  $121^\circ\text{C}$  ( $250^\circ\text{F}$ ) appear favorable.
- 7) Chlorine in the flue gas reduced the effectiveness of  $\text{Na}_2\text{S}_4$ -injection for gas-phase Hg-removal directly proportional to the concentration of chlorine in the flue gas.
- 8) Other than chlorine content,  $\text{Na}_2\text{S}_4$ -injection technology was unaffected by differences in coal-type or flue-gas composition for the conditions explored thus far.
- 9) While  $\text{Na}_2\text{S}_4$ -injection technology may be effective in the disperse phase (i.e., ESP applications),  $\text{Na}_2\text{S}_4$ -injection in front of a baghouse benefits from a residual effect, probably associated with the baghouse filter cake. Hence,  $\text{Na}_2\text{S}_4$ -injection in front of a baghouse may only require intermittent injection, and thus operational costs may be lower.

## Future Work

The present and previous results from this project thus far yield information from which the following future tests were conceived.

- 1) In order to directly measure the impact of UBC addition from bituminous ash on oxidized mercury capture by calcium, an experiment will be performed using dual baghouses. The first baghouse will be used to capture most of the ash and oxidize most of the mercury. The second baghouse will be used to test the effectiveness of  $\text{HgCl}_2$  capture by calcium, with and without bituminous ash and UBC present.
- 2) Sorbent development investigations are already underway to utilize the information obtained on UBC catalysis and mercury speciation. The composition of these designer sorbents will be optimized using the modified Catalyst Test Facility (CTF) at SRI. An optimized sorbent will be tested in the CRF to observe the ability of this designer sorbent to remove mercury in the disperse phase, through an ESP, and in a baghouse.

- 3) Advacate sorbent is specifically designed to remove SO<sub>2</sub> in a semi-dry recirculating system. This sorbent, high in UBC, will be examined for its effectiveness as a Multi-Pollutant Control Technology for removing both SO<sub>2</sub> and Hg from the flue gas.
- 4) Sodium tetrasulfide injection will be tested in the CRF for its ability to remove mercury across an ESP.
- 5) Finally, field-testing options will be explored for promising technologies.

## References

1. Gale, T. K., “Mercury Control with Calcium-Based Sorbents and Oxidizing Agents” Quarterly Report – DE-PS26-02NT41183 for period Oct. 1<sup>st</sup> through Dec. 31<sup>st</sup>, 2002.
2. Senior, C. L., Chen, Z., and Sarofim, A. F., “Mercury Oxidation in Coal-Fired Utility Boilers: Validation of Gas-Phase Kinetic Models”, *A&WMA 95<sup>th</sup> Annual. Conference.*, Baltimore MD, (2002).
3. Niksa, S., Helble, J. J., Fujiwara, N., “Kinetic Modeling of Homogeneous Mercury Oxidation: the importance of NO and H<sub>2</sub>O in predicting oxidation in coal-derived systems”, *Environ. Sci. Technol.*, **35**: 3701-3706 (2001).
4. Niksa, S., Fujiwara, N., Fujita, Y., Tomura, K., Moritomi, H., Tuji, T., and Takasu, S., “A Mechanism for Mercury Oxidation in Coal-Derived Exhausts” *J. A&WMA* **52**: 894-901 (2001).
5. Chen, Z., Senior, C. L., and Sarofim, A. F., “Modeling of Mercury States in Coal-Fired Utility Boilers” *27<sup>th</sup> Annual Technical Conference on Coal Utilization and Fuel Systems*, Clearwater Florida, March 4-7 (2002).
6. Niksa, S. and Helble, J. J., “Interpreting Laboratory Test Data on Homogeneous Mercury Oxidation in Coal-Derived Exhausts” *Fuel*, Submitted, 2002.
7. Lee, C. W., Kilgroe, J. D., and Ghorishi, S. B., “Speciation of Mercury in the Presence of Coal and Waste Combustion Fly Ashes”, *A&WMA’s 93<sup>rd</sup> Annual Conference and Exhibition*, Salt Lake City, UT (2000).
8. Niksa, S. and Fujiwara, N., “Predicting Mercury Speciation in Coal-Derived Flue Gases”, *EPRI-DOE-EPA-A&WMA Combined Utility Air Pollution Control Symposium: The MEGA Symposium*, May (2003).
9. Gale, T. K., “Mercury Control with Calcium-Based Sorbents and Oxidizing Agents” Quarterly Report – DE-PS26-02NT41183 for period Jan. 1<sup>st</sup> through Mar. 31<sup>st</sup>, 2003.

10. Licata, A., Schuttenhelm, W., and Klein, M., "Mercury Control for MWCs Using The Sodium Tetrasulfide Process", *8<sup>th</sup> Annual North American Waste-to-Energy Conference*, Nashville, TN, May 22 (2000).
11. Licata, A. and Fey, W., "Advanced Technology to Control Mercury Emissions", EPA-DOE-EPRI MEGA Symposium, Arlington Heights, IL, August (2001).
12. Norton, G. A., "Effects of Fly Ash on Mercury Oxidation During Post Combustion Conditions", Annual Report – DE-FG26-98FT40111 for period Sept 1<sup>st</sup>, 1999 through Aug. 31<sup>st</sup>, 2000.
13. Gale, T. K., Merritt, R. L., Cushing, K. M., and Offen, G. R., "Mercury Speciation as a Function of Flue Gas Chlorine Content and Composition in a 1 MW Semi-Industrial Scale Coal-Fired Facility", *EPRI-DOE-EPA-A&WMA Combined Utility Air Pollution Control Symposium: The MEGA Symposium*, May (2003).
14. Hurt, R. H. and Gibbins, J. R., "Residual Carbon from Pulverized Coal Fired Boilers: 1. Size Distribution and Combustion Reactivity", *Fuel* **74**(4): 471-480 (1995).
15. Gale, T. K., "Mercury Control with Calcium-Based Sorbents and Oxidizing Agents" Topical Report-DE-FC26-01NT41183 for period Sept. 5<sup>th</sup> 2001 through May 31<sup>st</sup> 2002.
16. US Patent 6,214,304 B1, 4/10/01, "Method of Removing Mercury from a Mercury-Containing Flue Gas", J. Rosenthal, W. Schuettenheim, M. Klein, R. Heidrich, U. Nikolai, U. Soldner, assignee L&C Steinmueller GmhH.



# APPENDIX A

## RUN CONDITIONS AND DATA

**Table A1.** Run conditions.

| Run # | Coal Type |     | Injection Condition                                                                          |
|-------|-----------|-----|----------------------------------------------------------------------------------------------|
|       | PRB       | CA  |                                                                                              |
| 1     | X         | --- | Unburned carbon test                                                                         |
| 2     | X         | --- | Unburned carbon test                                                                         |
| 3     | X         | --- | Unburned carbon test                                                                         |
| 4     | X         | --- | Unburned carbon test                                                                         |
| 5     | X         | --- | Unburned carbon test                                                                         |
| 6     | ---       | X   | Baseline Condition                                                                           |
| 7     | ---       | X   | Concentration of Na <sub>2</sub> S <sub>4</sub> in flue gas was 13.5 ppmv                    |
| 8     | ---       | X   | Raised flue-gas temperature, Na <sub>2</sub> S <sub>4</sub> in flue gas was 13.5 ppmv        |
| 9     | ---       | X   | Lowered flue-gas temperature, Na <sub>2</sub> S <sub>4</sub> in flue gas was 13.5 ppmv       |
| 10    | ---       | X   | Normal temperature, Na <sub>2</sub> S <sub>4</sub> in flue gas was 6.8 ppmv                  |
| 11    | ---       | X   | Na <sub>2</sub> S <sub>4</sub> in flue gas was 13.5 ppmv, repeat condition 2                 |
| 12    | ---       | X   | Inject chlorine through burner, Na <sub>2</sub> S <sub>4</sub> in flue gas was 13.5 ppmv     |
| 13    | ---       | X   | Half chlorine injection, Na <sub>2</sub> S <sub>4</sub> in flue gas was 13.5 ppmv            |
| 14    | ---       | X   | Maintain chlorine injection, turned off Na <sub>2</sub> S <sub>4</sub> injection             |
| 15    | X         | --- | Baseline                                                                                     |
| 16    | X         | --- | Concentration of Na <sub>2</sub> S <sub>4</sub> in flue gas was 12.2 ppmv                    |
| 17    | X         | --- | Concentration of Na <sub>2</sub> S <sub>4</sub> in flue gas was 6.1 ppmv                     |
| 18    | X         | --- | Return to Baseline                                                                           |
| 19    | X         | --- | Residual effect, concentration of Na <sub>2</sub> S <sub>4</sub> in flue gas was 2.9 ppmv    |
| 20    | X         | --- | Start fresh, concentration of Na <sub>2</sub> S <sub>4</sub> in flue gas was 2.9 ppmv        |
| 21    | X         | --- | Concentration of Na <sub>2</sub> S <sub>4</sub> in flue gas was 6.1 ppmv                     |
| 22    | X         | --- | Increased air-injection temperature, Na <sub>2</sub> S <sub>4</sub> in flue gas was 6.1 ppmv |
| 23    | X         | --- | Injection of over 400 ppm of SO <sub>2</sub> above air pre-heater                            |

CA = Choctaw America, PRB = Powder River Basin

**Table A2.** Run conditions continued.

| Run # | (@ 3% O <sub>2</sub> )<br>HCl in Flue Gas<br>(ppmv) | Baghouse<br>Temperature (°F)<br>Inlet-Outlet | FEO<br>(%) | Overfire<br>Air (%) | Coal Feed Rate<br>Lbs/hr |
|-------|-----------------------------------------------------|----------------------------------------------|------------|---------------------|--------------------------|
| 1     | 1.3 +/- 0.6                                         | 280-260                                      | 4.5        | 0                   | 364 +/- 3                |
| 2     | 1.3 +/- 0.6                                         | 280-260                                      | 3.5        | 15                  | 364 +/- 3                |
| 3     | 1.3 +/- 0.6                                         | 280-260                                      | 3.5        | 15                  | 364 +/- 3                |
| 4     | 1.3 +/- 0.6                                         | 280-260                                      | 1.5        | 26                  | 364 +/- 3                |
| 5     | 1.3 +/- 0.6                                         | 280-260                                      | 1.5        | 26                  | 364 +/- 3                |
| 6     | 9.8 +/- 0.5                                         | 300-273                                      | 4.5        | 15                  | 259 +/- 3                |
| 7     | 9.8 +/- 0.5                                         | 300-273                                      | 4.5        | 15                  | 259 +/- 3                |
| 8     | 9.8 +/- 0.5                                         | 375-325                                      | 4.5        | 15                  | 259 +/- 3                |
| 9     | 9.8 +/- 0.5                                         | 257-245                                      | 4.5        | 15                  | 259 +/- 3                |
| 10    | 9.8 +/- 0.5                                         | 303-275                                      | 4.5        | 15                  | 259 +/- 2                |
| 11    | 9.8 +/- 0.5                                         | 303-274                                      | 4.5        | 15                  | 259 +/- 3                |
| 12    | 84.6 +/- 4.5                                        | 303-274                                      | 4.5        | 15                  | 260 +/- 3                |
| 13    | 45.4 +/- 2.8                                        | 303-274                                      | 4.5        | 15                  | 259 +/- 3                |
| 14    | 45.4 +/- 2.8                                        | 304-273                                      | 4.5        | 15                  | 259 +/- 2                |
| 15    | 2.6 +/- 1.1                                         | 305-275                                      | 3.5        | 15                  | 364 +/- 3                |
| 16    | 2.6 +/- 1.1                                         | 306-275                                      | 3.5        | 15                  | 363 +/- 3                |
| 17    | 2.6 +/- 1.1                                         | 307-275                                      | 3.5        | 15                  | 364 +/- 3                |
| 18    | 2.6 +/- 1.1                                         | 308-275                                      | 3.5        | 15                  | 364 +/- 3                |
| 19    | 2.6 +/- 1.1                                         | 309-275                                      | 3.5        | 15                  | 364 +/- 3                |
| 20    | 2.6 +/- 1.1                                         | 310-276                                      | 3.5        | 15                  | 363 +/- 3                |
| 21    | 2.6 +/- 1.1                                         | 310-276                                      | 3.5        | 15                  | 364 +/- 3                |
| 22    | 2.6 +/- 1.1                                         | 310-276                                      | 3.5        | 15                  | 364 +/- 3                |
| 23    | 2.6 +/- 1.1                                         | 330-294                                      | 3.5        | 15                  | 363 +/- 3                |

**Table A3.** Mercury speciation measurements, corrected to 3% O<sub>2</sub> in flue gas.

| Run # | Hg <sup>T</sup> Mass Balance<br>$\mu\text{g}/\text{m}^3$ | Hg <sup>o</sup> /Hg <sup>T</sup> Baghouse Inlet (%) | Hg-Removal Baghouse Inlet (%) | Hg <sup>o</sup> /Hg <sup>T</sup> Baghouse Outlet (%) | Hg-Removal Baghouse Outlet (%) |
|-------|----------------------------------------------------------|-----------------------------------------------------|-------------------------------|------------------------------------------------------|--------------------------------|
| 1     | 8.4 +/- 0.8                                              | ---                                                 | ---                           | 78 +/- 2                                             | 12.7 +/- 3                     |
| 2     | 8.4 +/- 0.8                                              | ---                                                 | ---                           | 77 +/- 1                                             | 18.6 +/- 2                     |
| 3     | 8.4 +/- 0.8                                              | ---                                                 | ---                           | 74 +/- 2                                             | 15.7 +/- 3                     |
| 4     | 8.4 +/- 0.8                                              | ---                                                 | ---                           | 42 +/- 1                                             | 41.2 +/- 2                     |
| 5     | 8.4 +/- 0.8                                              | ---                                                 | ---                           | 56 +/- 8                                             | 45.1 +/- 8                     |
| 6     | 5.9 +/- 0.5                                              | 43 +/- 6                                            | ---                           | 0.0                                                  | 44 +/- 4                       |
| 7     | 5.9 +/- 0.5                                              | 77 - 97                                             | ---                           | 0.0                                                  | 90 +/- 2                       |
| 8     | 5.9 +/- 0.5                                              | 50 +/- 10                                           | ---                           | 0.0                                                  | 35 +/- 12                      |
| 9     | 5.9 +/- 0.5                                              | ---                                                 | 45.0                          | ---                                                  | 93 +/- 3                       |
| 10    | 5.9 +/- 0.5                                              | ---                                                 | ---                           | ---                                                  | 53 +/-11                       |
| 11    | 5.9 +/- 0.5                                              | ---                                                 | 14.6                          | ---                                                  | 74 +/-2                        |
| 12    | 5.9 +/- 0.5                                              | ---                                                 | 8.8                           | ---                                                  | 28 +/-14                       |
| 13    | 5.9 +/- 0.5                                              | ---                                                 | 1.7                           | ---                                                  | 56 +/-9                        |
| 14    | 5.9 +/- 0.5                                              | ---                                                 | ---                           | ---                                                  | 60 +/-5                        |
| 15    | 7.8 +/- 0.6                                              | 64 +/- 5                                            | 13.0                          | 39 +/- 5                                             | 43 +/-7                        |
| 16    | 7.8 +/- 0.6                                              | 100 +/- 5                                           | 33.0                          | ---                                                  | 99 +/- 2                       |
| 17    | 7.8 +/- 0.6                                              | ---                                                 | 35.0                          | ---                                                  | 100 +/- 2                      |
| 18    | 7.8 +/- 0.6                                              | ---                                                 | 19.0                          | ---                                                  | 75 +/- 2                       |
| 19    | 7.8 +/- 0.6                                              | ---                                                 | 26.0                          | ---                                                  | 90 +/- 2                       |
| 20    | 7.8 +/- 0.6                                              | ---                                                 | 17.0                          | ---                                                  | 70 +/- 4                       |
| 21    | 7.8 +/- 0.6                                              | ---                                                 | 23.0                          | ---                                                  | 88 +/- 9                       |
| 22    | 7.8 +/- 0.6                                              | ---                                                 | 27.0                          | ---                                                  | 92 +/- 2                       |
| 23    | 7.8 +/- 0.6                                              | ---                                                 | ---                           | ---                                                  | ---                            |

**Table A4.** Major flue gas species, corrected to 3% O<sub>2</sub> in the flue gas.

| Run # | NO <sub>x</sub><br>(ppm) | SO <sub>2</sub><br>(ppm) | CO<br>(ppm) | CO <sub>2</sub><br>(%) | (Actual)<br>O <sub>2</sub><br>(%) | H <sub>2</sub> O<br>(%) |
|-------|--------------------------|--------------------------|-------------|------------------------|-----------------------------------|-------------------------|
| 1     | 508 +/- 17               | 202 +/- 9                | 88 +/- 5    | 17.2 +/- 0.02          | 8.0 +/- 0.1                       | 9.8                     |
| 2     | 193 +/- 12               | 238 +/- 1                | 87 +/- 6    | 17.3 +/- 0.2           | 7.1 +/- 0.2                       | 9.8                     |
| 3     | 190 +/- 10               | 240 +/- 8                | 84 +/- 13   | 17.3 +/- 0.2           | 7.3 +/- 0.1                       | 9.8                     |
| 4     | 104 +/- 4                | 252 +/- 7                | 88 +/- 5    | 17.5 +/- 0.2           | 5.8 +/- 0.2                       | 9.8                     |
| 5     | 104 +/- 2                | 219 +/- 11               | 81 +/- 5    | 17.4 +/- 0.2           | 5.4 +/- 0.1                       | 9.8                     |
| 6     | 457 +/- 17               | 605 +/- 9                | 98 +/- 8    | 17.0 +/- 0.1           | 8.0 +/- 0.1                       | 7.2                     |
| 7     | 446 +/- 13               | 633 +/- 8                | 94 +/- 5    | 16.9 +/- 0.1           | 8.0 +/- 0.1                       | 7.2                     |
| 8     | 439 +/- 18               | 622 +/- 1                | 90 +/- 4    | 16.6 +/- 0.1           | 8.0 +/- 0.1                       | 7.2                     |
| 9     | 417 +/- 13               | 615 +/- 7                | 104 +/- 5   | 16.7 +/- 0.1           | 7.9 +/- 0.1                       | 7.2                     |
| 10    | 408 +/- 17               | 638 +/- 14               | 98 +/- 5    | 16.7 +/- 0.1           | 7.8 +/- 0.2                       | 7.2                     |
| 11    | 414 +/- 17               | 648 +/- 9                | 97 +/- 5    | 16.7 +/- 0.2           | 7.9 +/- 0.2                       | 7.2                     |
| 12    | 408 +/- 15               | 655 +/- 7                | 104 +/- 5   | 16.7 +/- 0.1           | 7.9 +/- 0.2                       | 6.3                     |
| 13    | 397 +/- 14               | 661 +/- 7                | 103 +/- 5   | 16.6 +/- 0.1           | 8.0 +/- 0.1                       | 6.5                     |
| 14    | 395 +/- 15               | 672 +/- 10               | 101 +/- 4   | 16.6 +/- 0.1           | 8.0 +/- 0.2                       | 7.2                     |
| 15    | 174 +/- 12               | 243 +/- 6                | 83 +/- 5    | 17.2 +/- 0.5           | 8.0 +/- 0.5                       | 9.9                     |
| 16    | 165 +/- 7                | 212 +/- 6                | 75 +/- 6    | 17.2 +/- 0.1           | 7.6 +/- 0.1                       | 9.9                     |
| 17    | 169 +/- 8                | 226 +/- 9                | 78 +/- 5    | 17.2 +/- 0.1           | 7.6 +/- 0.1                       | 9.9                     |
| 18    | 153 +/- 7                | 251 +/- 8                | 80 +/- 3    | 17.2 +/- 0.2           | 7.7 +/- 0.1                       | 9.9                     |
| 19    | 149 +/- 4                | 237 +/- 7                | 81 +/- 5    | 17.3 +/- 0.1           | 7.7 +/- 0.1                       | 9.9                     |
| 20    | 187 +/- 10               | 206 +/- 12               | 112 +/- 5   | 17.1 +/- 0.2           | 7.5 +/- 0.1                       | 9.9                     |
| 21    | 199 +/- 5                | 204 +/- 5                | 116 +/- 5   | 17.1 +/- 0.1           | 7.7 +/- 0.1                       | 9.9                     |
| 22    | 194 +/- 6                | 204 +/- 21               | 96 +/- 6    | 17.1 +/- 0.1           | 7.8 +/- 0.1                       | 9.9                     |
| 23    | 264 +/- 10               | 691 +/- 5                | 81 +/- 3    | 17.3 +/- 0.1           | 7.9 +/- 0.1                       | 9.9                     |

**Table A5.** Analysis of isokinetically sampled mass-train ash samples.

| Component                        | Run 1          | Run 2         | Run 3         | Run 4         | Run 5         |
|----------------------------------|----------------|---------------|---------------|---------------|---------------|
| % Li <sub>2</sub> O              | 0.02           | 0.02          | 0.02          | 0.02          | 0.02          |
| % Na <sub>2</sub> O              | 2.9            | 2.9           | 2.9           | 2.9           | 2.9           |
| % K <sub>2</sub> O               | 0.70           | 0.70          | 0.70          | 0.70          | 0.70          |
| % MgO                            | 5.4            | 5.4           | 5.4           | 5.4           | 5.4           |
| % CaO                            | 26.4           | 26.4          | 26.4          | 26.4          | 26.4          |
| % Fe <sub>2</sub> O <sub>3</sub> | 6.8            | 6.8           | 6.8           | 6.8           | 6.8           |
| % Al <sub>2</sub> O <sub>3</sub> | 19.0           | 19.0          | 19.0          | 19.0          | 19.0          |
| % SiO <sub>2</sub>               | 30.9           | 30.9          | 30.9          | 30.9          | 30.9          |
| % TiO <sub>2</sub>               | 2.0            | 2.0           | 2.0           | 2.0           | 2.0           |
| % P <sub>2</sub> O <sub>5</sub>  | 1.60           | 1.60          | 1.60          | 1.60          | 1.60          |
| % SO <sub>3</sub>                | 3.9            | 3.9           | 3.9           | 3.9           | 3.9           |
| % LOI                            | 0.42 +/- 0.07  | 0.28 +/- 0.06 | 0.28 +/- 0.06 | 0.43 +/- 0.02 | 0.43 +/- 0.02 |
| % UBC                            | 0.04 +/- 0.005 | 0.08 +/- 0.02 | 0.08 +/- 0.02 | 0.24 +/- 0.04 | 0.24 +/- 0.04 |

**Table A6.** Analysis of Baghouse ash samples.

| Component                        | Run 6         | Runs 7-9      | Runs 10-13    | Run 14        | Run 15        |
|----------------------------------|---------------|---------------|---------------|---------------|---------------|
| % Li <sub>2</sub> O              | 0.04          | 0.06          | 0.06          | 0.06          | 0.04          |
| % Na <sub>2</sub> O              | 1.3           | 2.5           | 2.5           | 1.95          | 2.1           |
| % K <sub>2</sub> O               | 1.5           | 1.9           | 1.9           | 1.95          | 1.6           |
| % MgO                            | 1.4           | 1.2           | 1.1           | 1.2           | 2.2           |
| % CaO                            | 12.9          | 6.4           | 4.5           | 5.4           | 10.4          |
| % Fe <sub>2</sub> O <sub>3</sub> | 14.2          | 11.6          | 12.4          | 11.9          | 10.5          |
| % Al <sub>2</sub> O <sub>3</sub> | 21.5          | 29.0          | 30.9          | 29.7          | 27.9          |
| % SiO <sub>2</sub>               | 36.6          | 40.02         | 41.9          | 41.6          | 39.2          |
| % TiO <sub>2</sub>               | 1.2           | 1.4           | 1.9           | 1.7           | 1.8           |
| % P <sub>2</sub> O <sub>5</sub>  | 0.42          | 0.38          | 0.38          | 0.4           | 0.67          |
| % SO <sub>3</sub>                | 8.7           | 4.6           | 3.9           | 4.05          | 3.7           |
| % LOI                            | 11.6          | 7.8           | 4.4           | 4.9           | 3.0           |
| % UBC                            | 6.34 +/- 0.05 | 5.32 +/- 0.04 | 2.79 +/- 0.02 | 3.13 +/- 0.24 | 1.93 +/- 0.02 |

**Table A7.** Analysis of Baghouse ash samples.

| Component                        | Run 16-19     | Runs 20-22    | Run 23        |
|----------------------------------|---------------|---------------|---------------|
| % Li <sub>2</sub> O              | 0.03          | 0.02          | 0.02          |
| % Na <sub>2</sub> O              | 2.7           | 2.5           | 2.5           |
| % K <sub>2</sub> O               | 0.75          | 0.63          | 0.63          |
| % MgO                            | 5.0           | 5.3           | 5.3           |
| % CaO                            | 25.3          | 28.1          | 28.1          |
| % Fe <sub>2</sub> O <sub>3</sub> | 7.8           | 6.6           | 6.6           |
| % Al <sub>2</sub> O <sub>3</sub> | 18.1          | 18.2          | 18.2          |
| % SiO <sub>2</sub>               | 31.2          | 31.1          | 31.1          |
| % TiO <sub>2</sub>               | 1.8           | 1.3           | 1.3           |
| % P <sub>2</sub> O <sub>5</sub>  | 1.3           | 1.4           | 1.4           |
| % SO <sub>3</sub>                | 4.7           | 3.7           | 3.7           |
| % LOI                            | 0.95          | 0.70          | 0.70          |
| % UBC                            | 0.35 +/- 0.00 | 0.16 +/- 0.00 | 0.16 +/- 0.00 |

**Table A8.** Mercury and sulfur in ash.

| Run # | Total Hg in Ash (μg/g) | <sup>a</sup> TCLP Hg in Extract (ppb) | Total TCLP-Hg Leached (wt%) <sup>c</sup> | <sup>b</sup> Sulfur in Ash (wt%) |
|-------|------------------------|---------------------------------------|------------------------------------------|----------------------------------|
| 1     | 0.025 +/- 0.010        | ---                                   | ---                                      | ---                              |
| 2     | 0.071 +/- 0.014        | ---                                   | ---                                      | ---                              |
| 3     | 0.071 +/- 0.014        | ---                                   | ---                                      | ---                              |
| 4     | 0.947 +/- 0.074        | ---                                   | ---                                      | ---                              |
| 5     | 0.947 +/- 0.074        | ---                                   | ---                                      | ---                              |
| 6     | 1.28                   | 20.6                                  | 0.0032                                   | 3.03                             |
| 7     | 1.94                   | 76.8                                  | 0.0079                                   | 2.53                             |
| 8     | 1.94                   | 76.8                                  | 0.0079                                   | 2.53                             |
| 9     | 1.94                   | 76.8                                  | 0.0079                                   | 2.53                             |
| 13    | 2.20                   | 69.9                                  | 0.0064                                   | 1.92                             |
| 14    | 1.84 +/- 0.28          | 70.4                                  | 0.0077                                   | 1.91 +/- 0.44                    |
| 15    | 1.76                   | 65.7                                  | 0.0075                                   | 1.78                             |
| 16    | 1.93                   | 0.342                                 | 0.000035                                 | 2.26                             |
| 17    | 1.93                   | 0.342                                 | 0.000035                                 | 2.26                             |
| 18    | 1.93                   | 0.342                                 | 0.000035                                 | 2.26                             |
| 19    | 1.93                   | 0.342                                 | 0.000035                                 | 2.26                             |
| 22    | 1.29                   | 30.5                                  | 0.0047                                   | 1.84                             |

a. The limiting concentration of mercury to pass the TCLP test is 200 ppb.

b. A measure of the volatile sulfur in the flyash, obtain by same method as ultimate analysis S.

c. Wt% = total Hg in ash/total mercury leached \* 100%.

## APPENDIX B

### SODIUM TETRASULFIDE INJECTION EQUIPMENT

Reagent supply. Sodium tetrasulfide was supplied by PPG Industries, Inc. as a nominal 34 wt% solution in water (PPG product ID 0068). The concentrated reagent was diluted to a 5.5 wt% solution with deionized water prior to injection. All tests at 100 and 50 mg/dscm injection rate used this solution directly. For the lowest injection rate tested, 25 mg/dscm, the solution was further diluted to 2.7% for injection. The dilute solution was also used for a 50 mg/dscm test. These injection rates are calculated concentrations of pure  $\text{Na}_2\text{S}_4$  in dry flue gas at 3%  $\text{O}_2$  and standard conditions (68 °F (20 °C), 1 atm.) in mg/dscm.

Figure B1 is a schematic of the solution metering and spraying system. Figure B2 shows photographs of the solution metering system and spray nozzle assembly. Dilute sodium sulfide solution is pumped out of the solution tank with a Cole-Parmer Micropump variable speed, magnetic drive gear pump, with most of the flow returned to the tank through a pressure regulating valve. The injection flow is metered with a Gilmont Instruments Accucal rotameter with a #215 tube and integral needle valve. The solution pressure to the nozzle (rotameter outlet) ranged from 20-40 psig.

Spray nozzle. A Spraying Systems Model 1/4JAC air-atomizing nozzle was used to spray the solution into the flue gas. The nozzle was located on the centerline of the 12" diameter flue gas duct, spraying co-currently with the flue gas. Air and solution were supplied to the nozzle through separate 3/8" SS tubes, which were also used to support the nozzle. The nozzle assembly can be seen in the lower left hand corner of Figure B2. The nozzle can be fit with a number of "spray setups", each setup consisting of a fluid cap and an air cap. Standard-spray setups are available with matched fluid and air caps for good atomization with an economic air/fluid ratio. These are interchangeable for customizing the nozzle performance. Nozzle configuration was not varied during these tests, but a combination of small fluid cap (#1650) and relatively large air cap (#1401110) was selected to obtain the finest possible spray in the small duct.

Atomizing air. Compressed air was supplied through a filter-regulator, rotameter, and needle valve. The air flowrate for all tests ranged from 3.5-4.5 scfm (16-20 lb/hr). For the baseline injection rate of 100 mg/dscm using 5.5 wt% sodium tetrasulfide, the solution injection rate was 36 ml/min (4.9 lb/hr), for an air/fluid ratio of 3.2-4.1 lb/lb. For injection rates of 50 mg/dscm (with 5.5% solution) or 25 mg/dscm (with 2.7% solution), the air/fluid ratio was about 7.6. The air pressure at the nozzle was about 30 psig.

Atomizing air heat. Atomization with steam, hot air, or hot flue gas has been reported to enhance the effectiveness of sodium tetrasulfide injection [16], particularly with lower-temperature flue gas. Steam was not available, but the air supply system included a 1200-watt heater and controller for preheating the atomization air. The heater was controlled using a thermocouple at the outlet of the heater, but another thermocouple mounted inside the air passage of the spray nozzle indicated the air temperature immediately before atomization. In the preliminary tests with gas firing, varying the atomizing air temperature (measured in the spray

nozzle) from 40-240 °C (100 to 460 °F) did not increase H<sub>2</sub>S formation from the decomposition of Na<sub>2</sub>S<sub>4</sub> (faster or more complete decomposition is expected to enhance reaction with mercury). Heating the atomizing air to 260 °C (500 °F) in the nozzle resulted in boiling within the nozzle and uncontrollable flow rate.

With coal firing and a baseline injection rate of 100 mg/dscm using 5.5 wt% solution, the atomizing air heater was controlled at 200 °C (390 °F), yielding an air temperature in the nozzle of 170-180 °C (340-360 °F) and a solution temperature in the nozzle of 45-65 °C (110-150 °F). At lower solution rates, the air temperature had to be decreased to avoid boiling within the nozzle. The effect of atomizing air temperature on mercury removal was not tested independently.

## Na<sub>2</sub>S<sub>4</sub> SOLUTION FLOW CONTROL PANEL

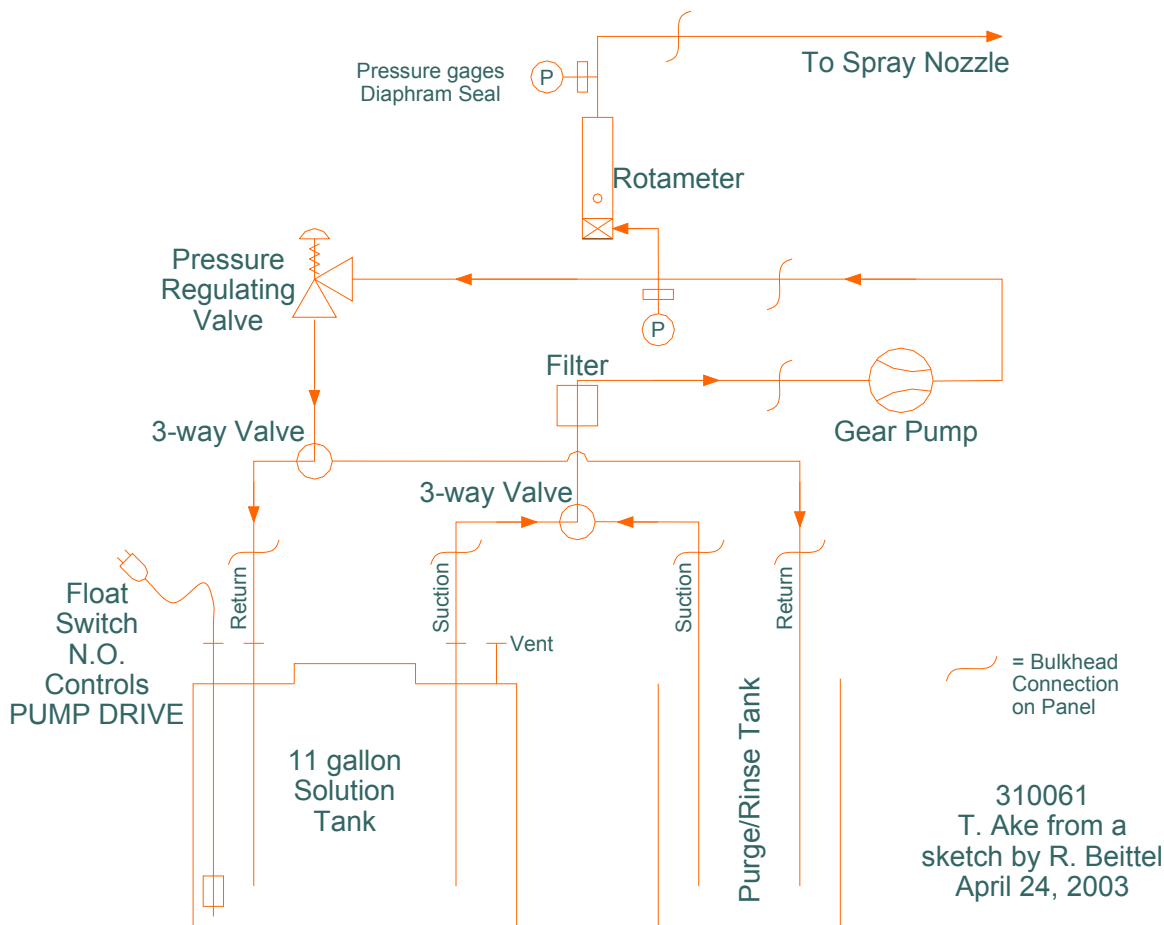


**Figure B1.** Sodium Tetrasulfide Injection Schematic.





**Figure B2.** Photographs of the sodium tetrasulfide injection system and spray nozzle assembly.

## APPENDIX C

### UBC VERSUS LOI

As has been shown in the present and previous [9] Quarterly Reports, unburned carbon (UBC) is a highly catalytic material, which is the most important factor in determining mercury speciation in coal-fired boilers. The test for UBC is by CHN analysis, the same analytical technique used to determine carbon, hydrogen, and oxygen for coal ultimate analysis. The resolution of this analytical technique is quite high. However, for most power plant characterization or operational data, UBC data is not available. Loss on ignition (LOI) is much more commonly used when characterizing power-plant operation, and LOI is obtained as part of the ash mineral analysis. Hence, modelers endeavoring to fit their model predictions with experimental data have desired to use LOI as an indicator of UBC or just to use LOI directly in their model instead of UBC [8].

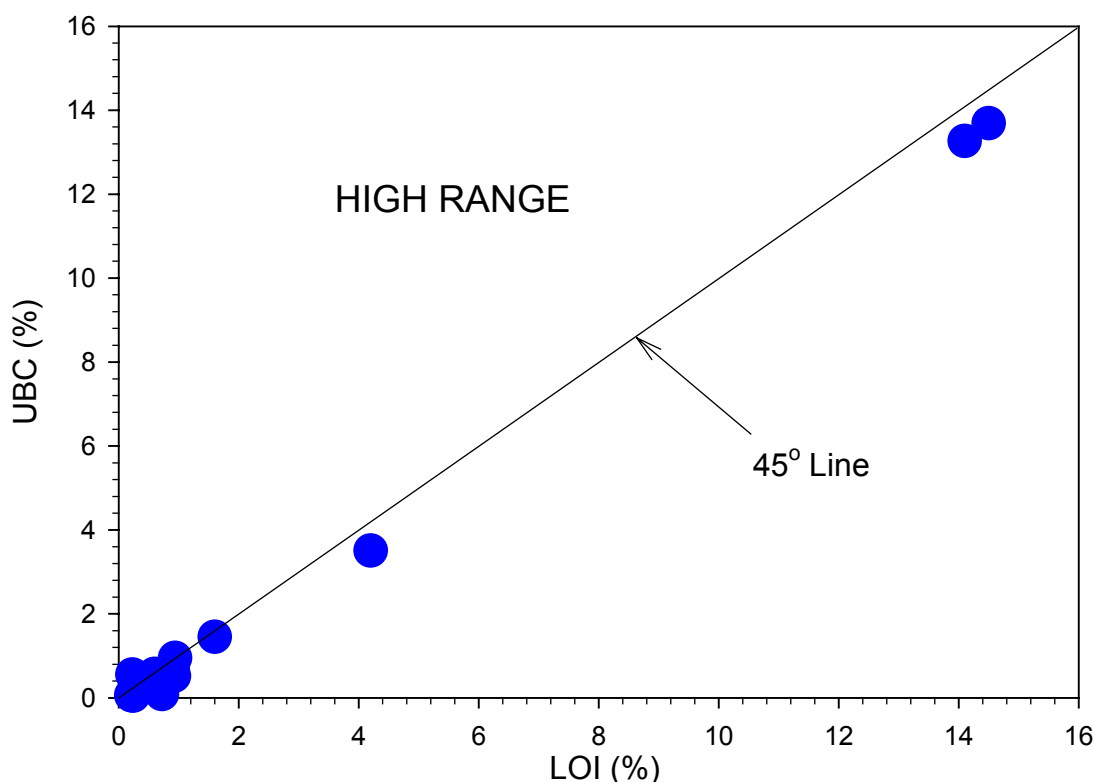


**Figure C1.** UBC versus LOI – high range.

Figure C1 illustrates the relationship between UBC and LOI for a large range, extending as high as 14% unburned carbon. As shown, the relationship between UBC and LOI is fairly consistent when observing this high data range. However, as shown in Fig. C2, for lower UBC and LOI in the ash, the relationship breaks down entirely. In fact, for the investigation presented in this and the previous [9] Quarterly Report, the majority of test conditions produced UBC levels below 1%. Therefore, if LOI had been used as an indicator of UBC for this investigation, *no relationship* between mercury speciation and UBC would have been shown. Consequently, when evaluating the UBC in ash to assess the probability of mercury capture across a baghouse

for high-burnout systems (i.e., most PRB coal burning plants), LOI should *NOT* be used to represent the UBC in the ash.

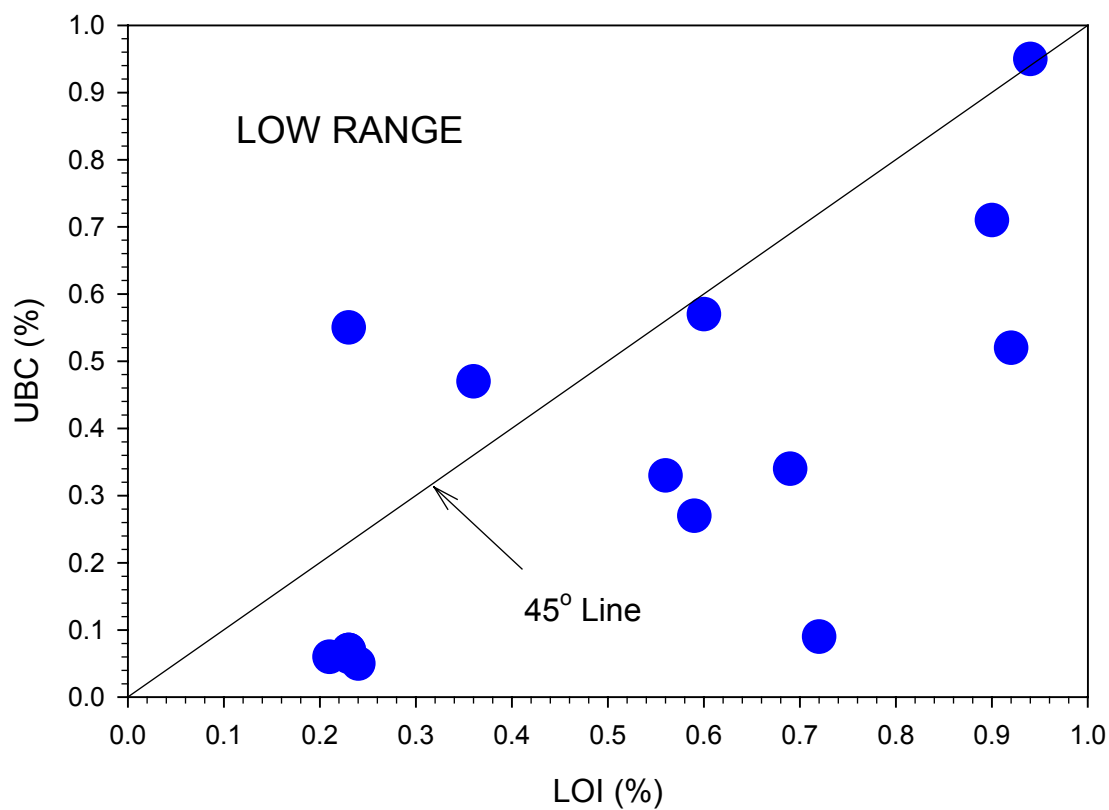


**Figure C2.** UBC versus LOI – low range.